THE JOURNAL OF COMPARATIVE NEUROLOGY 393:145–168 (1998)

Methionine Enkephalin Immunoreactivity in the Brain of the Budgerigar (*Melopsittacus undulatus*): Similarities and Differences With Respect to Oscine Songbirds

SARAH E. DURAND,* WENRU LIANG, AND STEVEN E. BRAUTH
Department of Psychology, University of Maryland, College Park, Maryland 20742-4411

ABSTRACT

The brain of the budgerigar (*Melopsittacus undulatus*), a small parrot that acquires new vocalizations throughout life, was examined for immunoreactivity to the opioid peptide methionine enkephalin (mENK). mENK is a highly prominent feature of the chemical architecture of the forebrain vocal system of oscine songbirds. Forebrain vocal control nuclei are believed to have evolved independently in parrots and songbirds (Streidter [1994] J. Comp. Neurol. 343:35–56); however, recent studies have found similarities in the neural organization of vocal control pathways in budgerigars and songbirds (Durand et al. [1997] J. Comp. Neurol. 377:179–206). Among the similarities are the existence of recursive pathways interconnecting vocal control neurons in the archistriatum, basal ganglia (i.e., lobus parolfactorius), and dorsal thalamus. In the present study, we found that all vocal control nuclei within the budgerigar forebrain exhibit prominent mENK-like immunoreactivity (ELI) in fibers and somata. We also found striking similarities between the morphology of ELI elements in budgerigar vocal control nuclei and that described previously in songbird vocal nuclei. Despite these similarities, the budgerigar dorsal striatopallidum (lobus parolfactorius, paleostriatum augmentatum, and paleostriatum primitivum) and somatomotor (anterior) archistriatum exhibit unique patterns of ELI. The dorsal striatopallidum contained far less ELI, whereas the archistriatum contained far more than would be expected on the basis of previous studies of opioid peptides in other avian species, including pigeons, chickens, and songbirds. These differences may reflect neural specializations unique to the budgerigar that contribute to the extraordinary flexibility of the vocal motor system of this species to acquire socially significant stimuli throughout life. J. Comp. Neurol. 393:145–168, 1998.

Indexing terms: opioid peptides; evolution; vocal learning; parrot; immunocytochemistry; psittacine

The neurobiology of vocal learning has been studied intensively in the oscine songbirds, a group of families in the Passeriformes order of perching birds (e.g., for reviews, see Nottebohm, 1991; Marler, 1991; Konishi, 1994; Bottjer and Arnold, 1997). Two other avian orders contain "vocal learners": The Trochiliformes (hummingbirds) and the Psittaciformes (parrots). The neurobiology underlying vocal learning in hummingbirds is unknown. Relatively few studies have examined the vocal control systems of parrots, an ancient lineage of birds with apparently no close relatives (Sibley and Ahlquist, 1990). However, vocal learning in some parrots resembles human vocal learning more closely than does song acquisition in oscines: The acoustic structure of acquired vocalizations in parrots is plastic and is highly susceptible to modification by social factors throughout life (Gramza, 1970; Pepperberg et al., 1991; Farabaugh et al., 1994; Banta and Pepperberg, 1995). Indeed, the argument has been made that acquisition of

Grant sponsor: National Institute for Deafness and Communication Disorders; Grant number: 5 F32 DC 00105-03; Grant sponsor: National Institute for Mental Health; Grant number: MH 40698.

*Correspondence to: Dr. S.E. Durand, Department of Psychology, University of Maryland, College Park, MD 20742-4411. E-mail: durand@bss3.umd.edu

Received 10 July 1997; Revised 5 November 1997; Accepted 6 November 1997

functional speech sounds by an African Gray Parrot resembles aspects of second-language learning in humans (Pepperberg, 1988).

The oscine species and the small parrot *Melopsittacus undulatus*, the budgerigar, possess a monosynaptic pathway from the telencephalon to medullary motor neurons that control vocal production (Nottebohm et al., 1976; Paton et al., 1981). However, anatomical and neurochemical data have suggested that the neural systems of the budgerigar pallium that support vocal learning evolved in part from neural populations different from those that comprise the pallial component of the songbird vocal system (Ball, 1994; Streidter, 1994; Durand et al., 1997). Unlike songbirds, auditory pathways into the vocal control system of the budgerigar (*M. undulatus*) were traced from the nucleus basalis (Streidter, 1994) and not from field L (the avian equivalent of primary auditory cortex; Karten, 1968), and a circuit through the anterior forebrain comparable to that mediating vocal learning in songbirds (Bottjer et al., 1984; Scharff and Nottebohm, 1991) was not identified in the budgerigar vocal system (Streidter, 1994). The neurochemistry of budgerigar vocal pathways has also appeared distinct: Although they are present in songbird vocal control nuclei (VCN), androgen receptors (Gahr et al., 1993), N-methyl-D-aspartic acid (NMDA) receptors (Ball and Casto, 1991), and α-adrenergic and muscarinic cholinergic receptors (Ball, 1990) have not been identified in budgerigar VCN (outside of the basal ganglia) with the techniques used to identify these proteins in songbirds.

More recent findings, however, point to important similarities in vocal forebrain organization between oscines and budgerigars, suggesting that, although vocal learning evolved independently in oscines and psittacines (cf. Streidter, 1994), important functional parallels exist nevertheless. First, like songbirds, budgerigars possess pathways that interconnect nuclei of the anterior neostriatum, paleostriatum, and dorsal thalamus with premotor neurons of the archistriatum (Durand et al., 1997). Some of these pathways resemble the anterior forebrain circuit of oscines, although additional circuits through the budgerigar hyperstriatum apparently do not have counterparts in the oscine song system. Second, two lines of evidence suggest that thalamotelencephalic auditory pathways have direct connections with the budgerigar vocal system: 1) The thalamorecipient auditory field L in the budgerigar has been demonstrated to project onto a region of the anterior neostriatum (Farabaugh and Wild, 1997) that was proposed by Streidter (1994) to be afferent to the primary vocal-motor pathway from the archistriatum. 2) Retrograde tracing from the vocal control nucleus of the hyperstriatum labeled cells not only within the abovementioned region of the anterior neostriatum but also within field L (Durand et al., 1996, 1997). Thus, auditory input may reach the VCN of the budgerigar from both

Abbreviations

AAa	anterior nucleus of anterior archistriatum
AAc	central nucleus of anterior archistriatum
AAcd	dorsal subdivision of central nucleus of anterior archistriatum
AAcv	ventral subdivision of central nucleus of anterior archistriatum
AAm	medial nucleus of anterior archistriatum
AAv	ventral region of anterior archistriatum
Ac	nucleus accumbens
AC	anterior commissure
AL	ansa lenticularis
Am	nucleus ambiguus
APH	area parahippocampus
ArC	archiastriatum centrale
Area X	area X of lobus parolfactorius
ArM	archiastriatum mediale
Ar	archistriatum posterioris
AVT	area ventralis
Bas	nucleus basalis
BNST	bed nucleus of the stria terminalis
CoS	nucleus of the septal commissure
CP	posterior commissure
DIP	dorsointermediate nucleus of posterior thalamus
DLL	dorsolateral nucleus of anterior thalamus, lateral part
DM	dorsomedial nucleus of nucleus intercollicularis
DMm	magnocellular nucleus of dorsomedial thalamus
DSD	dorsal supraoptic decussation (decussation supraoptic dorsalis)
E	ectostriatum
FPL	lateral forebrain bundle (fasciculus prosencephali lateralis)
HA	accessory hyperstriatum
HD	dorsal hyperstriatum
HIS	hyperstriatum intercalatus superior
Hp	hippocampus
HV	ventral hyperstriatum
HVo	oval nucleus of ventral hyperstriatum
ICC	central nucleus of inferior colliculus
ICo	intercollicular nucleus
ICX	external nucleus of inferior colliculus
Imc	isthmic nucleus, magnocellular part
INP	intrapeduncular nucleus
Ipc	isthmic nucleus, parvocellular part
L2	lamina 2 (thalamorecipient) of field L
LAD	dorsal archistriatal lamina
LFS	superior frontal lamina (lamina frontalis superior)
LH	hyperstriatal lamina
LMD	dorsal medullary lamina (lamina medullaris dorsalis)
LoC	locus ceruleus
LPO	lobus parolfactorius
LPOm	magnocellular nucleus of lobus parolfactorius
ME	median eminence of hypothalamus
N	neostriatum
NA	neostriatum anterior
NAo	oval nucleus of anterior neostriatum
NAom	medial division of the oval nucleus of anterior neostriatum
NC	caudal neostriatum
NI	intermediate neostriatum
nIII	nucleus of oculomotor nerve
NIVL	intermediate neostriatum, ventrolateral part
NL	lateral neostriatum
NLc	central nucleus of lateral neostriatum
NLs	supracentral nucleus of lateral neostriatum
NLv	ventral nucleus of lateral neostriatum
nX	dorsal motor nucleus of the vagus nerve
nXII	hypoglossal nucleus
OM	occipitomesencephalic tract
OT	optic tectum
Ov	ovoid nucleus of thalamus
PA	paleostriatum augmentatum (augmented paleostriatum)
PMH	medial nucleus of posterior hypothalamus
POA	preoptic area
PP	paleostriatum primitivum (primitive paleostriatum)
PrV	principal sensory nucleus of trigeminal nerve
PT	pretectal nucleus
Rt	rotund nucleus
S	septum
SGP	periventricular gray substance of tectum
Sl	septum, lateral part
Sm	septum, medial part
SMe	stria medullaris
SN	substantia nigra
SpL	lateral spiriform nucleus
Tn	nucleus taeniae
TSM	septomesencephalic tract (tractus septomesencephalicus)
VCN	vocal control nuclei
VP	ventral paleostriatum

thalamic and nonthalamic sources. Finally, a nucleus within the budgerigar hyperstriatum, the oval nucleus of the ventral hyperstriatum (HVo; Streidter, 1994), has been shown to be an integral component of both the newly identified anterior forebrain vocal circuits and the previously described descending motor pathway (Durand et al., 1996, 1997). The connections of the HVo are comparable to those of the songbird neostriatal "high vocal center" (HVC or HVc; for review, see Margoliash et al., 1994), in that both nuclei are positioned to direct premotor neuronal activity: Whereas the HVC projects a nontopographic and massive input directly onto the archistriatum, the HVo projects a massive nontopographic projection onto the lateral neostriatum directly afferent to the archistriatum (Durand et al., 1996, 1997). Both the HVC and the HVo also project upon two rostrolateral populations of the basal ganglia (avian "striatum") that share a similar histochemistry and hodology (Ball, 1994; Streidter, 1994).

Thus, despite differences in some aspects of anatomical organization, forebrain vocal control systems of budgerigars and oscines exhibit important organizational similarities. A recent histochemical study (Cookson et al., 1996) revealed that, as in oscines, forebrain vocal nuclei in budgerigars exhibit enhanced staining for cholinergic markers relative to surrounding neuronal fields, thereby pointing to another feature of organization common to the design of two presumably nonhomologous neural systems that serve vocal learning.

In the present study, nuclei proposed to constitute anterior forebrain circuits in the budgerigar vocal system and nuclei of the primary motor pathway to the syrinx were examined for methionine enkephalin-like immunoreactivity (ELI). Double-labeling experiments, in which tissue labeled with an anatomical tracer (Durand et al., 1997) was processed for immunocytochemistry, were also performed to determine the pattern of association of reactive fibers and projection neurons. Additional brain regions for which ELI is described in some detail include the paleostriatal complex (avian basal ganglia), the archistriatum, and nuclei of the diencephalon and mesencephalon that have been identified as immunoreactive for mENK in other avian species (Bayon et al., 1980; de Lanerolle et al., 1981; Reiner et al., 1982b, 1984, 1989; Durand et al., 1993).

We chose to study mENK immunoreactivity in the budgerigar because of the ubiquity of this particular opioid peptide in the vocal control pathways of all oscine songbird species studied to date. Apparently, all VCN of the songbird forebrain contain conspicuous ELI terminal fields (Ryan et al., 1981; Ball et al., 1988; Bottjer and Alexander, 1995). Given the considerable independence that appears to have occurred in the evolution of vocal learning in songbirds and budgerigars, we can make the following argument: Features of neural organization in the budgerigar forebrain that are similar to the specialized neural connections mediating song control in songbirds may be those features that are essential to socially mediated motor learning. According to this reasoning, the results presented here indicate that an essential feature of neural connections controlling the social acquisition of vocal-motor behavior is their modulation by an opioid peptide.

MATERIALS AND METHODS

The subjects of this study were 15 adult budgerigars, seven males and eight females, and one 3-week-old nestling. The birds were housed in a free-flight, walk-in aviary equipped with perches of variable diameter and objects that could be manipulated or climbed. Seeds, fresh water, greens, and minerals were supplied daily. In all but two cases (an adult male and the 3-week-old subject), the birds that served the immunocytochemistry experiments were also subjects of tract-tracing experiments (Durand et al., 1997): Individuals received either iontophoretic injections of tracers that could be visualized with a peroxidase reaction (see below), or they received pressure injections of tracers that were conjugated with a fluorescent tag (rhodamine). Survival periods following injection of a tracer ranged from 10 hours to 2 weeks. Colchicine was not used to enhance somal labeling. In a previous study (Durand et al., 1993), intraventricular injections of colchicine in doves prior to mENK immunocytochemistry resulted in greatly diminished fiber labeling and did not alter the assessment of ELI distribution, although greater numbers of somata were stained. Animals that received the injections appeared to experience intense discomfort. Finally, a recent study that examined ELI in a songbird in the absence of colchicine pretreatment (Bottjer and Alexander, 1995) reported more extensive somal label than that seen in earlier studies in which the drug was used (Ryan et al., 1981; Ball et al., 1988).

All subjects were killed with an overdose of sodium pentobarbitol (78 mg/bird) and were perfused transcardially or through the carotid arteries with 30–75 ml of 1.5% dextran in 0.8% saline followed by 100 ml of 4.0% paraformaldehyde in 0.1 M phosphate-buffered saline (PBS), pH 7.2. Brains were removed from the skull and either were placed first in the fixative (postfixation times varied from 12 hours to 24 hours) or were placed directly into a cryoprotectant (25% sucrose in PBS) for 24–48 hours. In one exceptional case, sections were treated for immunocytochemistry after remaining in the fixative for approximately 2 weeks. These sections were compared with equivalent sections from other cases. Unexpectedly, no decrement in the relative intensity of staining was observed in this case. Tissue was then sectioned on a sliding microtome at 40 μm. Tissue sections were collected serially in 0.02 M potassium PBS, pH 7.4 (KPBS). In only one case (an adult male) were all sections used for immunocytochemistry; in 13 cases, sections were taken every 80–120 μm; in 2 cases, only sections containing VCN were used.

After sections were collected, they were either first incubated in 1.0% H_2O_2 for 10 minutes and washed four times for 5 minutes each (five cases), or they were washed once in KPBS and placed directly into the primary antiserum solution: Primary antiserum against mENK raised in rabbit (Incstar Corp., Stillwater, MN) was diluted 1:1,000–1:8,000 in KPBS with 3% normal goat serum (NGS) and 0.3% Triton X-100. Following 48–72 hours in the primary antiserum under gentle agitation at 4°C, the sections were washed six times for 10 minutes each and were incubated at room temperature for 2–3 hours under gentle agitation in either 1) biotinylated goat anti-rabbit serum (Vector Laboratories, Burlingame, CA) diluted 1:100–1:300 in KPBS with 2% NGS or 2) or in a fluorescein-tagged goat anti-rabbit serum at a dilution of 1:50 in KPBS/NGS.

The choice of fluorescent tag or chromagen for visualizing immunoreactive cellular elements was based on its usefulness in distinguishing these elements from material stained with an anatomical tracer (see above). In the cases where immunoreactivity was visualized with the fluores-

cein tag (three adult females), sections were washed four times for 10 minutes each in KPBS and then wet mounted onto slides in KPBS, pH 8.6, for observation with the fluorescein exciter filter of a Zeiss Axioplan microscope (Thornwood, NY). In the cases incubated with the biotinylated secondary antibody (all others), sections were washed three times for 10 minutes each in KPBS with 1% NGS and then four times for 10 minutes each in KPBS prior to placement in a KPBS solution containing avidin and biotinylated peroxidase (as provided by the Vector Elite Standard "A" and "B" solutions at a dilution of two drops per 30 ml; Vector Laboratories) with 1% bovine serum albumin. Following a 1–2 hour incubation in the peroxidase solution at room temperature, sections were washed five times for 10 minutes each in KPBS and were stained for 2–5 minutes in a solution of 0.003% H_2O_2 in KPBS with one of three chromagen solutions: 0.04% 3′,3-diaminobenzidene tetrahydrochloride (Sigma Chemical Co., St. Louis, MO) or the Vector SG or VIP chromagens (Vector Laboratories) at the recommended kit dilutions. Stained sections were washed four times for 10 minutes each in either KPBS or dH_2O and then mounted onto gelatin-coated slides, dried, dehydrated, cleared, and mounted under glass coverslips.

After an initial analysis of the stained material, coverslips were removed from selected slides, and the sections were rehydrated for subsequent intensification of the reaction product with silver and gold impregnation, according to the protocol of Kitt et al. (1994). Some of this intensified material was counterstained with the Nissl stain neutral red, so that immunoreactive cellular elements could be viewed in conjunction with surrounding somal profiles. Selected sections were photographed through a Zeiss Axoplan microscope. The resulting negatives were digitized at 2,025 dpi (35-mm scanner; Polaroid, Inc., Cambridge, MA) by using Adobe PhotoShop (Adobe Photoshop, Inc., Mountain View, CA). Gray-scale files were printed on a 300-dpi, dye-sublimation printer (Phaser 440 color printer; Tektronix, Beaverton, OR), and color files were printed on an ink jet printer (DeskJet 870Cxi; Hewlett-Packard, Corvallis, OR) at 300 dpi.

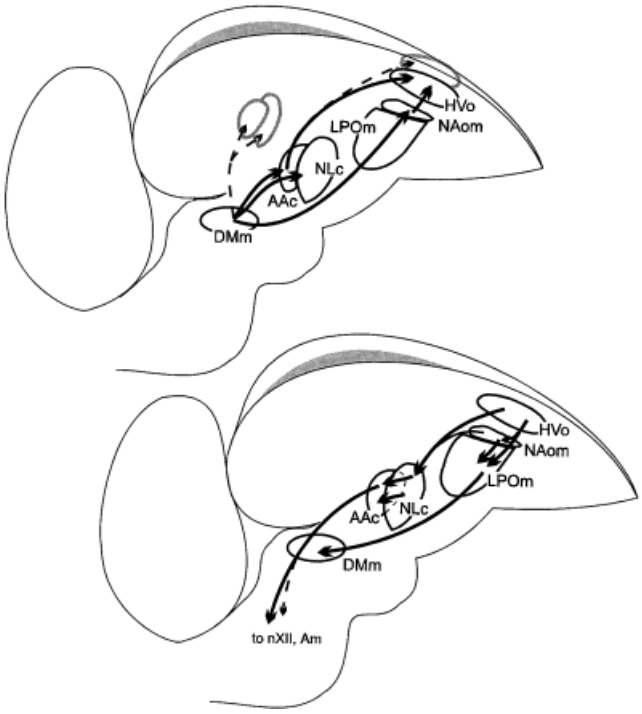

Fig. 1. Schematic drawings in the sagittal plane illustrate the interconnections between the forebrain vocal control nuclei (VCN) of the budgerigar. The **top** drawing indicates ascending connections, and the **bottom** drawing indicates descending connections. Note that, compared with the VCN of oscine songbirds, the connections of the budgerigar VCN form more numerous "looped" pathways, some of which are restricted to the pallium. Several loops interconnect nuclei of the primary descending pathway (central nucleus of the lateral neostriatum [NLc] and central nucleus of the anterior archistriatum [AAc]) with nuclei of the anterior forebrain (oval nucleus of the ventral hyperstriatum [HVo] and medial division of the oval nucleus of the anterior striatum [NAom]). For other abbreviations, see list.

RESULTS

Individual and sex differences

The observed patterns of ELI staining did not vary with sex. However, this study does not address possible quantitative differences in ELI distribution between males and females. Photomicrographs are derived from both male and female cases and are identified accordingly. There was variation in both cell body and terminal field staining across cases, and case variability was as great within as it was between sexes. In two males and one female, terminal fields were labeled only weakly, and it was necessary to examine the tissue at high power in order to visualize fiber labeling. Nevertheless, staining patterns in these cases were not different from those observed in other cases. In the cases of another male and female, background staining associated with the chromagen SG was sufficiently high to obscure somal ELI except in regions of intense cellular reactivity.

To illustrate the similarity of ELI staining patterns in males and females, immunoreactive cells and fibers are depicted within the central nucleus of the neostriatum (NLc) in both a male and a female (see NLc, below). This nucleus was selected for comparing males and females because of its distinctive and heterogeneous distribution of reactive elements.

ELI staining was mapped in one nestling in order to compare the distribution of reactive terminal fields in an immature forebrain vocal system with the distribution of ELI fields in the adult VCN. Although staining of terminal fields was clear in this case, somal labeling was weak, and reactive somata could be identified readily only within the basal forebrain.

Methionine ELI fibers: An overview

The distribution of ELI in the budgerigar brain generally resembled patterns reported for other avian species (see Discussion, below). However, there were three striking features in the pattern of telencephalic ELI: 1) Reactive fields were present within all cell groups identified as VCN (Figs. 1, 2), 2) exceptionally high reactivity was distributed throughout the archistriatum, and 3) very low reactivity was present within the dorsal striatopallidum (Fig. 2, PP, paleostriatum primitivum). Reactive fibers were present in all telencephalic VCN thus far identified: The NLc and the central nucleus of the anterior archistriatum (AAc); the oval nuclei of the ventral hyperstriatum and the anterior neostriatum (NAo), medial portion (HVo

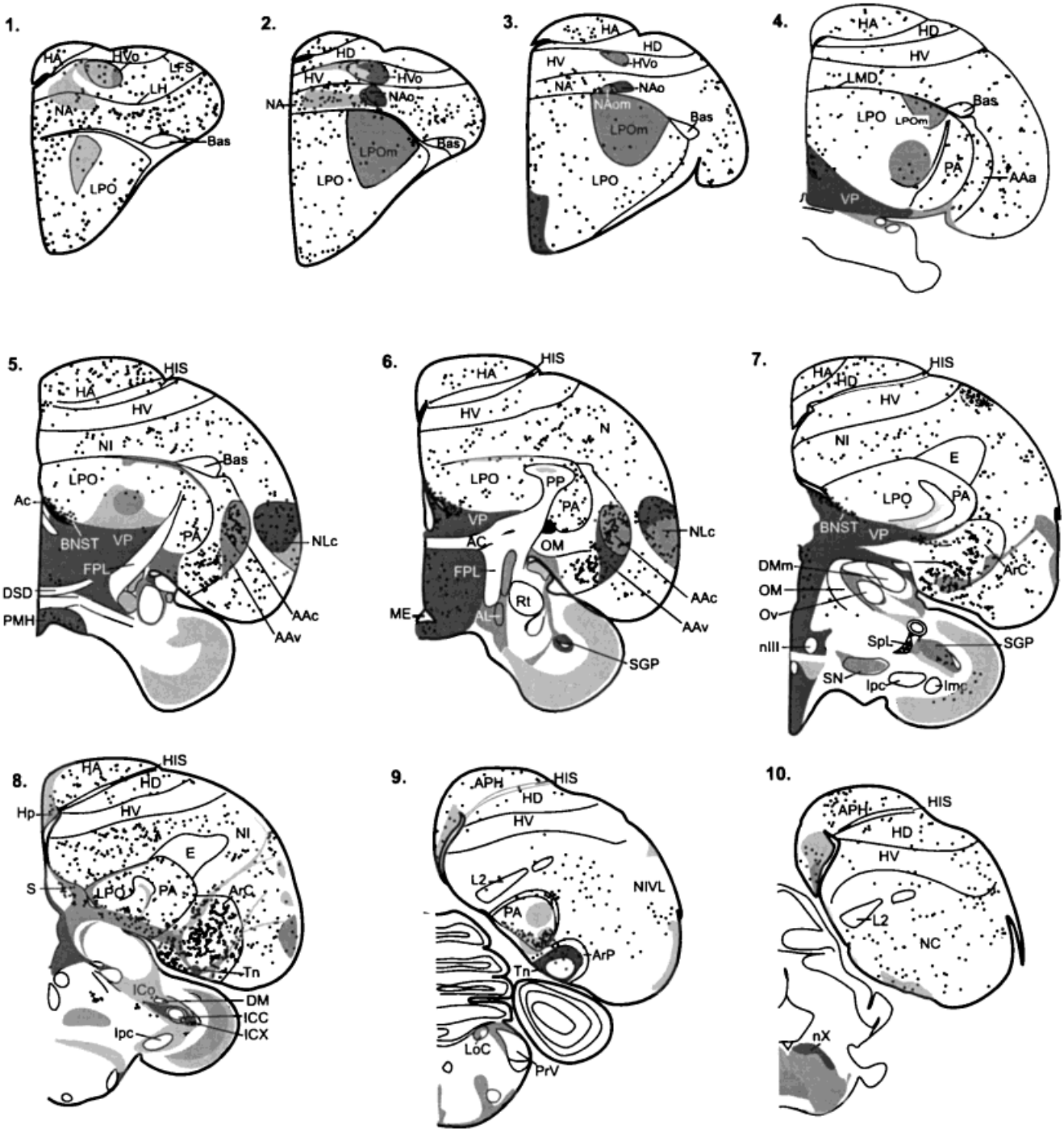

Fig. 2. **1–10:** Series of camera lucida drawings in the transverse plane arranged in rostral-to-caudal sequence illustrates patterns of methionine enkephalin-like immunoreactivity (ELI) in the budgerigar brain. Dots indicate the location of individual stained somata. ELI fiber fields are represented in shades of gray, with relative abundance of stained fibers indicated by gradations in shading intensity (darkest shade indicates highest density). Drawings were made from an adult male. All photomicrographs in the figures that follow are displayed in the above orientation unless otherwise noted. For abbreviations, see list.

and NAom, respectively); and the magnocellular portion of the LPO (LPOm). In each case, the associated reactive field extended beyond the Nissl-defined boundary of the vocal control nucleus in one or more directions (see Fig. 2 [5–8] for lateral VCN; see Fig. 2 [1–5] for anterior VCN). Thus, reactive fields completely filled the telencephalic VCN and, in some sections, were congruent with the boundaries of these nuclei (see, e.g., Fig. 2 [3,6]). Outside the VCN-associated fields, few reactive fibers were present within neostriatal and hyperstriatal areas (however, see Fig. 2 [7–9]).

In contrast, medial, ventral, and caudal populations of the paleostriatum exhibited intense reactivity, although the paleostriatum primitivum (PP) did not (see below and Discussion). Midline populations of the diencephalon were intensely reactive (Fig. 2 [5–8]), including the preoptic area, hypothalamus, and median eminence. The central portions of most thalamic nuclei exhibited little reactivity, although high concentrations of reactive fibers surrounded many of these nuclei.

Within the midbrain (Fig. 2 [6–8]), intensely stained axonal fields were present within periventricular populations of the tectum. These reactive fields extended medially into the intercollicular region and the midbrain central gray and extended ventrally into the underlying reticular formation. Nuclei associated with the basal ganglia, the substantia nigra and area ventralis of Tsai, contained reactive fibers. The locus ceruleus and the dorsal and ventral subceruleus also appeared to receive enkephalinergic input. Within the pons, the magnocellular region of the reticular formation was devoid of ELI, but scattered reactive fibers were present in more lateral parvocellular populations and also surrounded the motor nuclei of the trigeminal and facial nerves. Reactive fields within the pontine reticular formation extended caudally into the medulla. The latter brain region was most notable for the intense staining of the dorsal motor nucleus of the vagus.

Methionine ELI somata: An overview

Reactive neurons with elliptical or spherical profiles of $<$12 μm were distributed widely throughout the telencephalon (Fig. 2), with the exception of rostral dorsal hyperstriatum (HD), caudal ventral hyperstriatum (HV), and primary sensory fields of the neostriatum: the ectostriatum, field L, and the nucleus basalis. 1) All telencephalic VCN identified in previous work (Fig. 1) contained reactive cells of this type (Fig. 2 [1–3,5,6]). 2) In some regions of the neostriatum, the numbers of reactive cells exceeded those of PA and LPO (e.g., Fig. 2 [1,2], NA). Cells within PA and LPO were generally similar in size (approximately 10 μm) and morphology to reactive cells in overlying telencephalic areas. 3) Reactive somata were more abundant within the archistriatum than within PA and LPO at all levels (Fig. 2 [4–9]), except for localized regions within peripheral portions of the PA and LPO, where reactive cells were packed more densely, noticeably larger (12–15 μm), and stained darker. High levels of stained perikarya were present throughout the archistriatum, including both the caudomedial (amygdaloid) and the rostrolateral (somatomotor) subdivisions (Zeier and Karten, 1971; Veenman et al., 1995). Many cells were also labeled in the lateral septal nucleus, ventral striatum (nucleus accumbens), and bed nucleus of the stria terminalis (BNST). Cell profiles within the latter three cells were quite large ($>$20 μm).

Within the diencephalon, reactive somata were generally restricted to the hypothalamus, median eminence, and preoptic area. Within the pretectum, the lateral spiriform nucleus (SpL; Fig. 2 [7]) contained numerous large (25–30 μm) reactive somata. Smaller cells were clustered along the margins of the central nucleus of the inferior colliculus (torus) and were sparsely scattered within the intercollicular region (Fig. 2 [8]). More densely distributed and larger cells were present within the periaqueductal gray. In the ventral thalamus, scattered reactive cells were intermingled with fibers of the occipitomesencephalic tract (OM) and extended into regions just medial to the OM.

VCN

Reactive fields that encompassed the telencephalic VCN (NLc, AAc, HVo, NAo, and LPOm) are shown in darkfield at low magnification in Figure 3. The density of reactive elements was greatest within the NAo and was lowest within the core region of the LPOm (Fig. 3B). Within the NLc, AAc, and HVo, reactive fibers were not distributed homogeneously. The dorsal portion of the NLc contained a dense fiber network. The ventral NLc contained a patchy distribution of reactive fibers, thereby giving the region a punctate appearance (Fig. 3A). Within the AAc, fiber density was greatest within the medial periphery of the nucleus. Within the HVo, fiber density decreased from lateral to medial portions of the nucleus.

None of the reactive fields within the VCN was strictly confined to the anatomically identified boundaries of these nuclei (see Fig. 1 in Durand et al., 1997). However, the abundance of reactive elements, as visualized in coronal sections, was always greatest within the boundaries of each nucleus. Labeled varicose fiber segments could be traced between the AAc and the NLc and between the LPOm, the NAo, and the HVo. The reactive fiber fields of both the anterior and lateral VCN were continuous with labeled fields of the basal forebrain (Figs. 4, 5), suggestive of immunoreactive axonal projections into the VCN (see Discussion).

Widely scattered, varicose fibers extended from the AAc, across the archistriatal lamina, and into the narrow strip of neostriatum between the AAc and the NLc (Fig. 4A). Reactive fields associated with the NLc and AAc extended beyond the Nissl-defined caudal and ventral boundaries of these nuclei. Caudal to the NLc, a tapering field of stained fibers extended as far as the level of caudal PA, thereby forming an end zone to the NLc field proper (Figs. 2 [7–9]). The fiber clusters that distinguished the NLc field were not present in this caudal end zone (Fig. 4A). However, discrete dorsal and ventral regions could still be distinguished relative to reactive fields that were separated by a nonimmunoreactive zone (Fig. 2 [8]) before diminishing to a narrow strip of labeled fibers within the subventricular region of the caudal neostriatum (Fig. 2 [9]). An immunoreactive field also extended from the AAc into more caudal and ventral portions of the archistriatum. This area caudal to the AAc proper could be followed more caudally until it merged with a region of extremely high reactivity within the nucleus taeniae (Tn), which, itself, was continuous with a smaller and more loosely organized field within the medial archistriatum (Figs. 2 [7,8], 4B). All of these archistriatal fields were continuous with the medially adjacent fields of the ventral paleostriatal complex. Long segments of arching varicose axons were observed extending from the laterally adjacent BNST and the ventral paleostriatum (VP) into the region identified as the Tn (Fig. 2 [8]; see also Fig. 4B, Tn).

The reactive fields of the HVo, NAo, and LPOm were also interconnected by scattered varicose fibers. Both coarse and fine-caliber axons extended between the LPOm and the overlying NAo (Fig. 5A). Likewise, widely scattered fibers extended across the hyperstriatal lamina between the NAo and the HVo (Fig. 5B). Fields within the latter

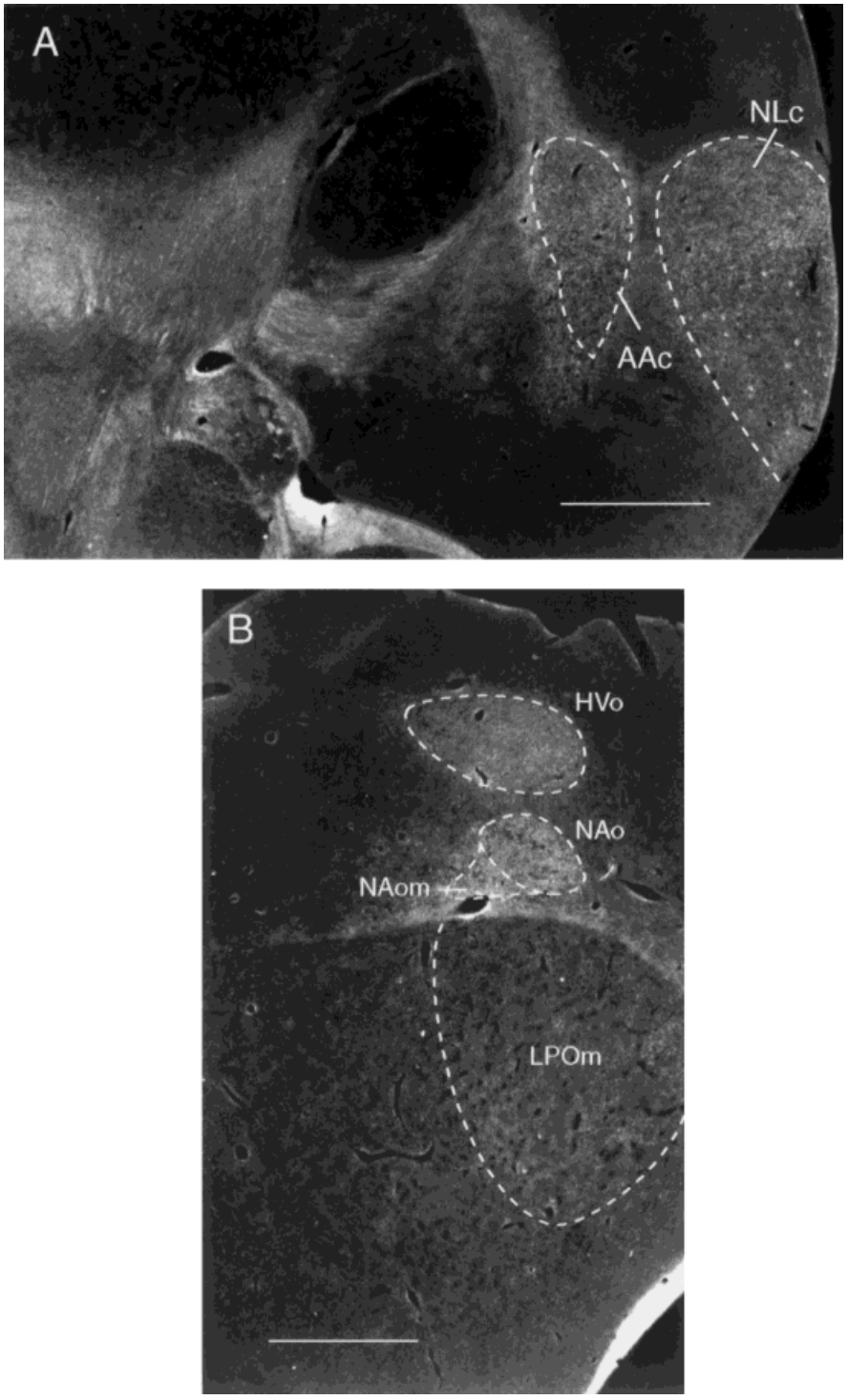

Fig. 3. **A:** Darkfield photomicrograph illustrates enkephalin-like immunoreactivity (ELI) patterns within the lateral vocal control nuclei (VCN), central nucleus of anterior archistriatum (AAc), and central nucleus of lateral neostriatum (NLc). Boundaries of nuclei are indicated by dashed lines. Bright areas indicate fiber tracts and ELI fiber plexuses. Note that the ELI plexus in the AAc extends across the medial and ventral boundaries of the nucleus. **B:** Darkfield photomicrograph illustrates ELI fiber plexuses within the anterior VCN, oval nucleus of ventral hyperstriatum (HVo), medial division of the oval nucleus of anterior neostriatum (NAom), and magnocellular nucleus of the lobus parolfactorius (LPOm). Note that the ELI plexus in the NAo covers the full extent of the nucleus and extends beyond its medial boundary. Subject was male in A and B. Scale bars = 1 mm.

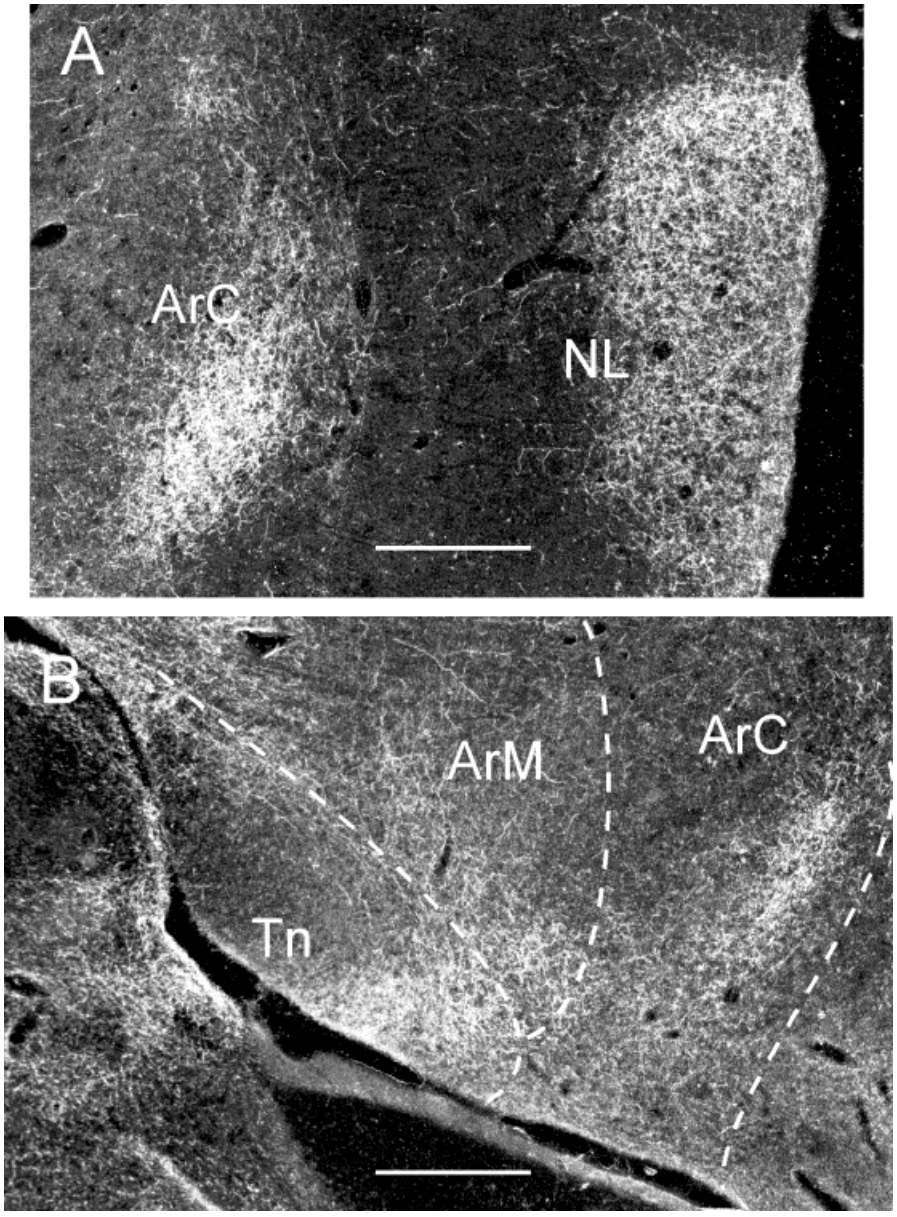

Fig. 4. Two darkfield photomicrographs. **A:** Enkephalin-like immunoreactivity (ELI) fibers within the central archistriatum (ArC) and within an undefined region of lateral neostriatum (NL), populations continuous with the caudal boundaries of central nucleus of lateral neostriatum (NLc) and central nucleus of anterior archistriatum (AAc, see Fig. 3). Note the unbranching ELI fibers that span the neostriatum interposed between the two fiber plexuses. These fields are continuous with the ELI fields shown in B. Dotted line indicates the location of the dorsal archistriatal lamina (LAD). **B:** Darkfield photomicrograph of ELI fiber plexuses in the archiastriatum mediale (ArM), the ArC, and the nucleus taeniae (Tn): Archistriatal regions are outlined by dashed lines. The level depicted is caudal and ventral to that shown in A. Note that ELI fibers in the somatomotor ArC appear to merge with plexuses in ventral fields, such as nucleus taeniae (Tn). Subject was male in A and B. Scale bars = 500 μm.

nuclei were also continuous along their rostromedial pole (Fig. 2 [1]).

NLc. The strikingly nonhomogeneous distribution of reactive elements within the NLc is demonstrated for both sexes in Figure 6; tissue from the male (Fig. 6A) was counterstained, whereas the female tissue was not (Fig. 6B). The dorsal portion of the NLc is characterized by a more densely distributed fiber plexus relative to central and ventral regions of the nucleus. The punctate appearance of the ELI within ventral portions of the NLc, which is prominent in the counterstained tissue of the male, is revealed at high magnification to be associated with clusters of varicose fibers in both sexes (Fig. 6C,D, female subject; Fig. 7, male subject). Within the dorsal NLc (Fig. 6C), these fiber clusters are considerably smaller than those of similar morphology that occur within more ventral regions (Fig. 6D), although the latter are embedded within a more loosely organized fiber plexus. When examined in the counterstained tissue of the male subject (Fig. 7), the fiber clusters appear to form perikaryal baskets that surround Nissl-stained profiles. High-power magnification of the ventral perikaryal baskets reveals their

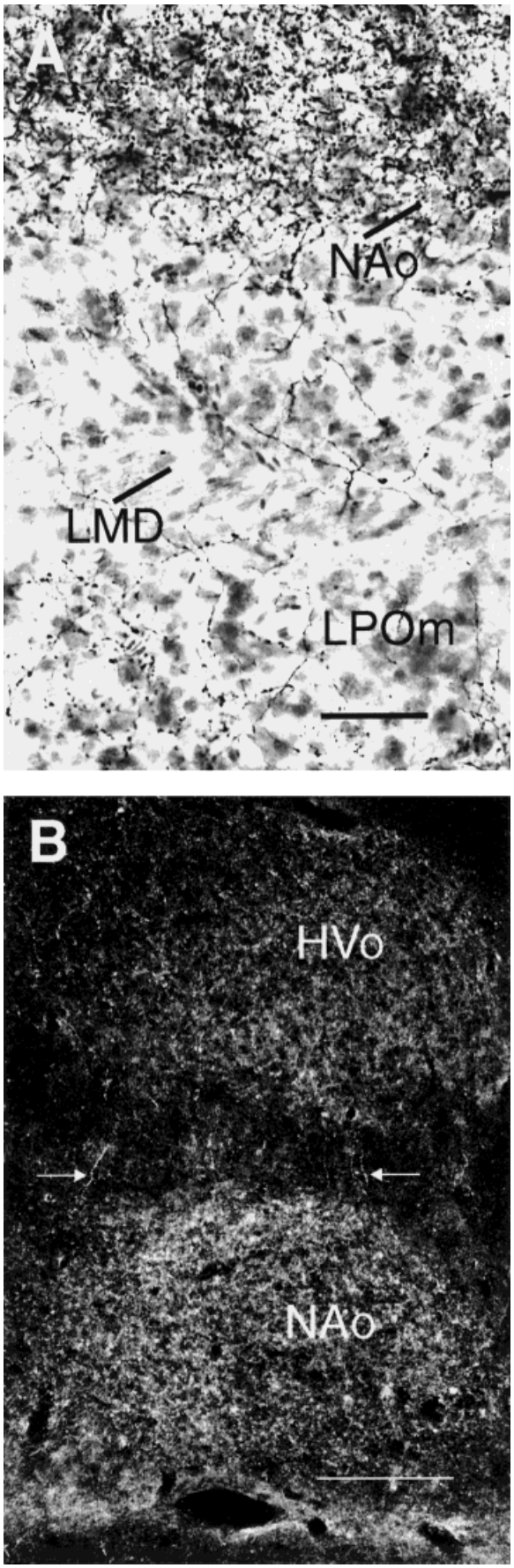

association with more than one Nissl-stained profile (Fig. 7B) compared with the single profiles associated with baskets of the dorsal NLc. The association of ventral baskets with several Nissl-stained profiles accounts for their prominence in Nissl-stained material. In both regions of the NLc, the fiber clusters were larger than reactive neurons (approximately 12 μm; Fig. 7A), which were scattered throughout the nucleus.

AAc. The highest density of reactive neurons among the VCN was observed within the AAc (Fig. 8). This observation was consistent with the finding that the archistriatum contained the highest density of reactive cells within the pallium (see above). No perikaryal clusters of reactive fibers were observed here, although varicose fibers overlay somatic profiles en passant within medial portions of the nucleus. Within the lateral dorsal and ventral subdivisions of the AAc, fiber varicosities were most prevalent in the interstices between somatic profiles, so that the Nissl-stained profiles appeared to lie in the openings of a loosely organized fiber network. Reactive fibers appeared to accumulate along the medial boundary of the AAc, and the field within the AAc was continuous with fields in the immediately adjacent archistriatum, medial and ventral to AAc.

HVo. The density of fiber labeling within the lateral HVo was greater than that within central and medial regions of the nucleus (Fig. 9A,B). Although varicosities were associated with somal profiles in counterstained tissue, few well-defined varicose clusters were observed (Fig. 9B). Fewer reactive neurons were present within the HVo than within the NLc, but relatively more were present within the HVo than in the surrounding hyperstriatum (Figs. 2 [1,2], 9A). Reactive fibers extended from the medial pole of the HVo, along the superior frontal lamina (LFS), toward the midline. Some fibers extended across the LFS into the HD, where widely scattered reactive somata were distributed along the lamina.

NAo. Immunoreactive cells were more abundant in the neostriatum surrounding the NAo than within the nucleus itself (Figs. 2 [2], 9A). The neostriatum medial to the NAo contained a particularly high density of reactive cells. The high density of labeled fibers within the NAo made it difficult to visualize stained fiber terminals in relation to Nissl-stained profiles, although it appeared that clusters of varicosities were particularly abundant over Nissl-stained somata (Fig. 9C). No reactive somata were observed within the central NAo, although stained somata were visible within the dorsolateral and medial (NAom) portions of the nucleus (note that only the NAom has been identified anatomically as a component of VCN pathways; Durand et al., 1997).

mENK immunoreactivity in a 3-week-old nestling. The morphology of reactive fields within the AAc and HVo of the 3-week-old subject was broadly similar to what was observed in adults (Fig. 10A,D). However, the NLc and NAo contained reactive fields that differed from the adult

Fig. 5. **A:** Nissl-stained material in brightfield with enkephalin-like immunoreactivity (ELI) fibers extending through the fiber tract (dorsal medullary lamina; LMD) that runs between the oval nucleus of anterior neostriatum (NAo) and the lobus parolfactorius (LPOm), nuclei that contain ELI fiber plexuses. **B:** ELI fiber plexuses in darkfield within the oval nucleus of ventral hyperstriatum (HVo) and NAo; arrows indicate fibers traversing the hyperstriatal lamina (LH), the lamina situated between the NAo and the HVo. Subject was male in A and B. Scale bars = 100 μm in A, 500 μm in B.

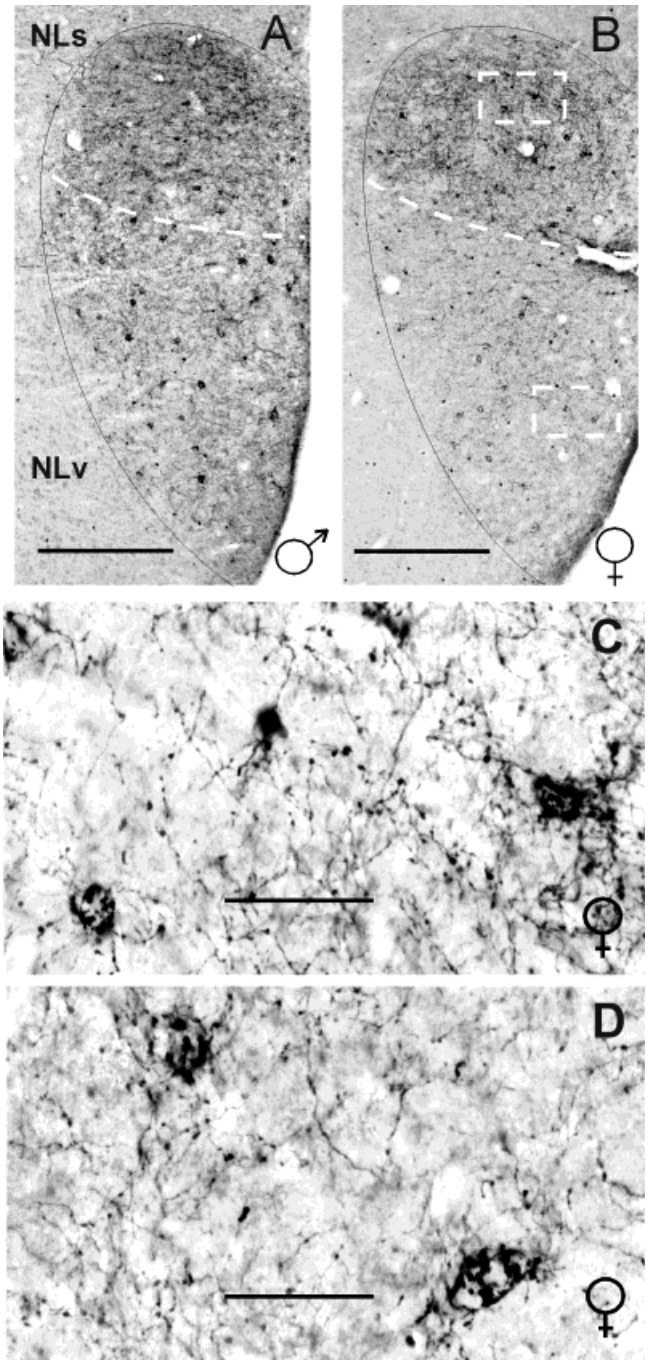

Fig. 6. Brightfield photomicrographs with the boundaries of the central nucleus of lateral neostriatum (NLc) outlined in black. **A:** Nissl-stained tissue from a male. Note the nonhomogeneous pattern of ELI distribution in the NLc with respect to the dorsal and ventral portions of the nucleus. Particularly intense punctate staining of ventral NLc is evident. **B:** Tissue from a female that was not treated with Nissl stain exhibits similar nonhomogeneous distribution of ELI fibers in the NLc, but the punctate staining of the ventral NLc is less prominent. **C:** At higher magnification, the female dorsal NLc reveals clusters of varicose fibers ("baskets") embedded in a fiber network (a poorly focused ELI soma is also visible). **D:** In the female ventral NLc, fiber clusters of noticeably larger size are present, and surrounding fibers are distributed less densely. NLs, supracentral nucleus of the lateral neostriatum; NLv, ventral nucleus of the lateral neostriatum. Scale bars = 500 μm in A,B, 50 μm in C,D.

with respect to the internal pattern of fiber distribution. Within the NLc (Fig. 10A,B), basket-like clusters of reactive fibers were not observed within either dorsal or ventral portions of the nucleus. Similar to the adult, the density of reactive fibers was greater in the dorsal NLc, and fibers were observed outside of the boundaries of the immature nucleus, within the neostriatal tissue lying between the NLc and the anterior archistriatum. These peripheral fibers appeared to be fine-caliber varicose axons. The densely distributed reactive field within the nestling NAo (Fig. 10C) was a bipartite structure: A relatively nonreactive strip of tissue was interposed between the main body of a densely distributed, reactive field and a more loosely organized medial portion (Fig. 10C; see also Discussion).

LPOm. A relatively diffuse field of reactive fibers was present throughout the LPOm (Figs. 5, 17D). Most of the fibers within the LPOm field were oriented vertically along the plane of section, although reactive fibers formed a plexus subadjacent to the dorsal medullary lamina (LMD) that forms the dorsal boundary of the LPO. Contrary to the pattern observed for other VCN, reactive somata were less abundant within the LPOm than within surrounding tissue. The end zone of the fiber field, caudal to the LPOm, extended as far caudally as the level of the AAc (Fig. 2 [5]). At this level, two discrete fiber fields were present within the LPO. One was a field that occupied the ventrolateral LPO, and the other field was much smaller and was subadjacent to the LMD (see Figs. 2 [5], 15C). Immunostained fibers could be traced between these two fields. The LPOm end zone contained many more reactive cells than the LPOm field proper. In addition, these cells were larger and were stained darker (Fig. 15C).

Magnocellular portion of the dorsomedial nucleus of the thalamus. A very few fine fibers and sparsely distributed puncta were present within the thalamic vocal control nucleus, the magnocellular portion of the dorsomedial nucleus of the thalamus (DMm; Figs. 2 [7], 11A). Puncta were generally localized to Nissl profiles of the magnocellular neurons of the nucleus (Fig. 11A). No reactive somata were observed. The low density of stained elements within this nucleus contrasts with a high density of reactive fibers within structures along the dorsal and ventral periphery of the DMm, respectively, the stria medullaris and the shell region of the auditory thalamus (Fig. 11B). Fine fibers could be followed from the stria into the underlying DMm.

Dorsomedial nucleus of the mesencephalon and intercollicular area. A region of reduced reactivity was present dorsomedial to the rostral pole of the toral central nucleus (Fig. 11C). This region overlapped a weak projection of the AAc (Fig. 11D) that was identified previously (Durand et al., 1997), and its relative position corresponded to that of the dorsomedial nucleus of the intercollicular region (DM), identified in the pigeon (Wild and Arends, 1987). Fine, beaded fibers coursed through the nucleus parallel to its long axis. Large varicosities generally overlay Nissl profiles, but clusters of puncta were not observed. The region directly ventrolateral to the DM (Fig. 11C), identifiable by a particularly high density of reactive fibers, corresponded in position to the core and shell portions of the intercollicular area, as distinguished by Puelles et al. (1994) on the basis of high immunoreactivity to leucine enkephalin.

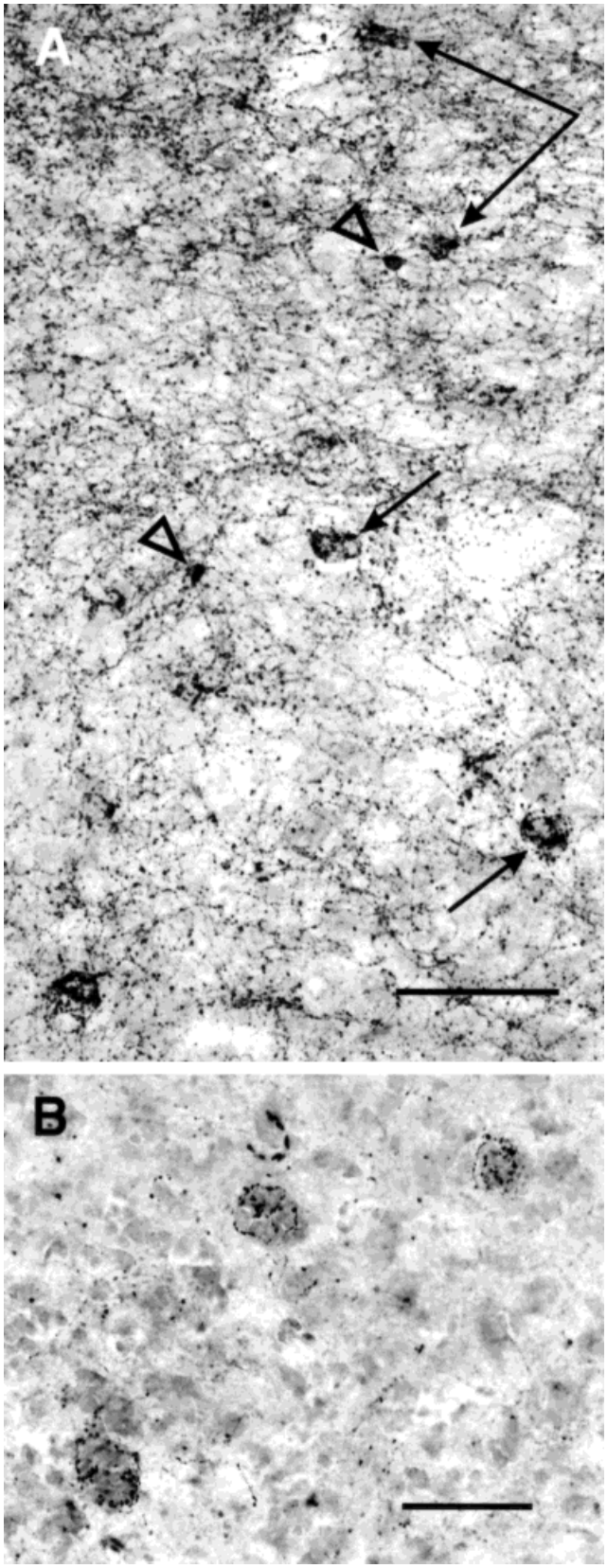

Pallial fields external to those associated with vocal control pathways

Immunoreactive cells and fibers were present within the hippocampus (Hp: Figs. 2 [8–10], 12A). Parallel nonvaricose fibers extended from the Hp into the subventricular zone throughout the anteroposterior extent of this structure. Ventral and caudal areas of the Hp contained a moderately dense network of fine, varicose fibers and many reactive somata.

Along the lateral rim of the NL, dorsal and caudal to the reactive fields associated with the NLc, reactive fibers congregated below the lamina hyperstriatica. Reactive somata appeared slightly larger within this field relative to stained cell bodies within the surrounding neostriatum (Figs. 2 [6–9], 12B).

Paleostriatum and archistriatum

The concentration of reactive somata within the archistriatum was generally greater than that within dorsal populations of the basal ganglia, i.e., the PA and the LPO (Figs. 2 [5–9], 13). This result was unexpected in view of previous studies (see Discussion). The relatively low density of reactive somata within the LPO and PA was associated with the absence of a well-defined field of reactive fibers within the PP, a target population of the PA (Karten and Dubbeldam, 1973; Fig. 14A–C). The rostral and central PP contained occasional scattered fibers; caudal to the ectostriatum, loosely distributed reactive fibers were present throughout the caudal pole of the PP (Fig. 14C). Reactive somata within the ventrolateral PA were also most abundant at these levels (see below). Although reactivity was unexpectedly low within the PA and the PP, the SpL of the pretectum in receipt of PP projections contained large reactive somata (Fig. 14D), and the tectum contained numerous reactive fibers (Fig. 2 [5–8]; see also Fig. 16D).

Within small, localized areas of the PA and LPO, concentrations of reactive somata approached the levels observed in the archistriatum. These areas included the ventral and ventrolateral margins of the PA (especially its caudal pole; Figs. 13, 14C), the end zone of the LPOm reactive field (Fig. 15C), and the medial margin of the LPO (Fig. 16A). Immunostained cells within the LPOm end zone were larger and more darkly stained relative to reactive cells within the surrounding LPO. Subpallial populations of the medial telencephalon, including the nucleus accumbens, the BNST (Fig. 15B), and the lateral septum (Fig. 16A), contained high concentrations of reactive cells and fibers, whereas the ventral paleostriatum and the nucleus of the septal commissure contained abundant reactive fibers but few reactive somata (Fig. 16B).

Fig. 7. High-magnification brightfield photomicrographs of Nissl-stained material from a male. **A:** Enkephalin-like immunoreactivity (ELI) somata (arrowheads) and fiber clusters (arrows) are present. Clusters exhibit a size variation similar to clusters within the female NLc; dorsal clusters (linked arrows) are small relative to clusters in ventral NLc (single arrows). All fiber clusters are present in association with Nissl-stained profiles, thus forming perikaryal baskets. **B:** Higher magnification of ELI elements in the ventral NLc reveals that large ELI fiber baskets enclose several Nissl-stained cellular profiles, accounting for the prominent punctate appearance of the ventral NLc in Figure 6A. Scale bars = 100 μm in A, 50 μm in B.

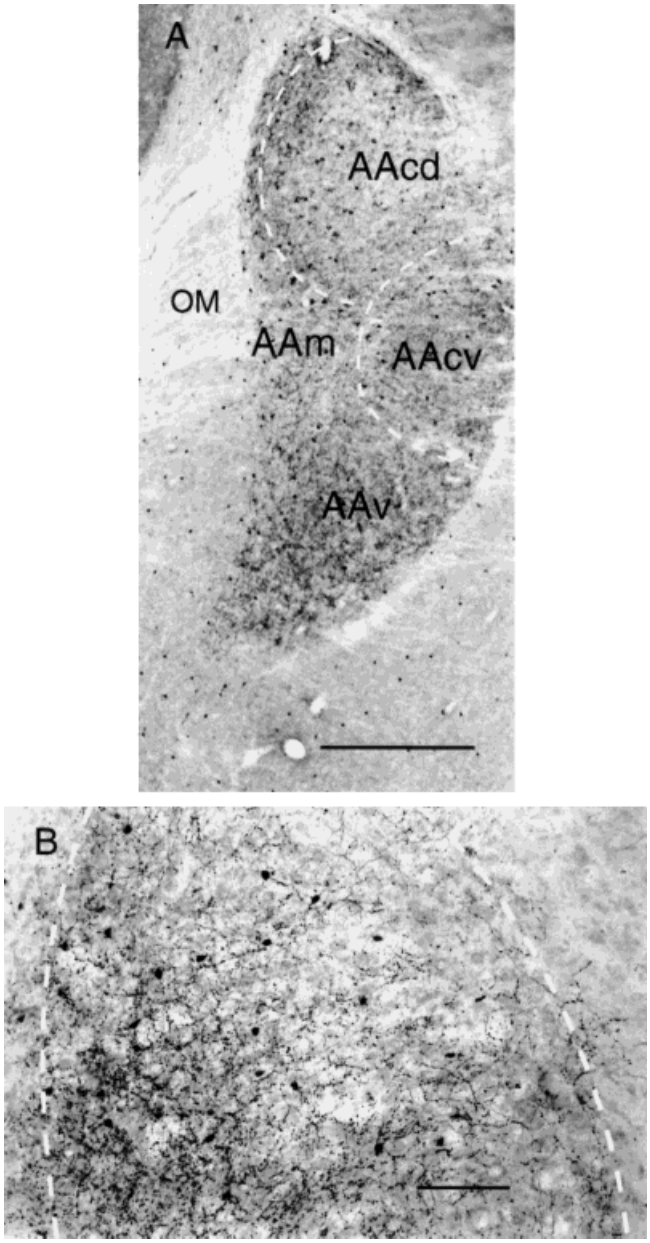

Fig. 8. Brightfield photomicrographs illustrate patterns of enkephalin-like immunoreactivity (ELI) staining in the anterior archistriatum. **A:** ELI fields extend beyond the AAc (dorsal subdivision [AAcd] and ventral subdivision [AAcv]; dashed lines indicate boundaries defined by Nissl staining) and into the medial nucleus of the anterior archistriatum (AAm) and the ventral region of the anterior archistriatum (AAv). **B:** Higher magnification of the AAc (within the dashed outline) reveals that the lateral AAcd contains less fiber labeling and fewer stained somata than other parts of the AAc. Note that fibers appear to congregate along the medial border of this nucleus. Subject was female in A and B. Scale bars = 500 μm in A, 100 μm in B.

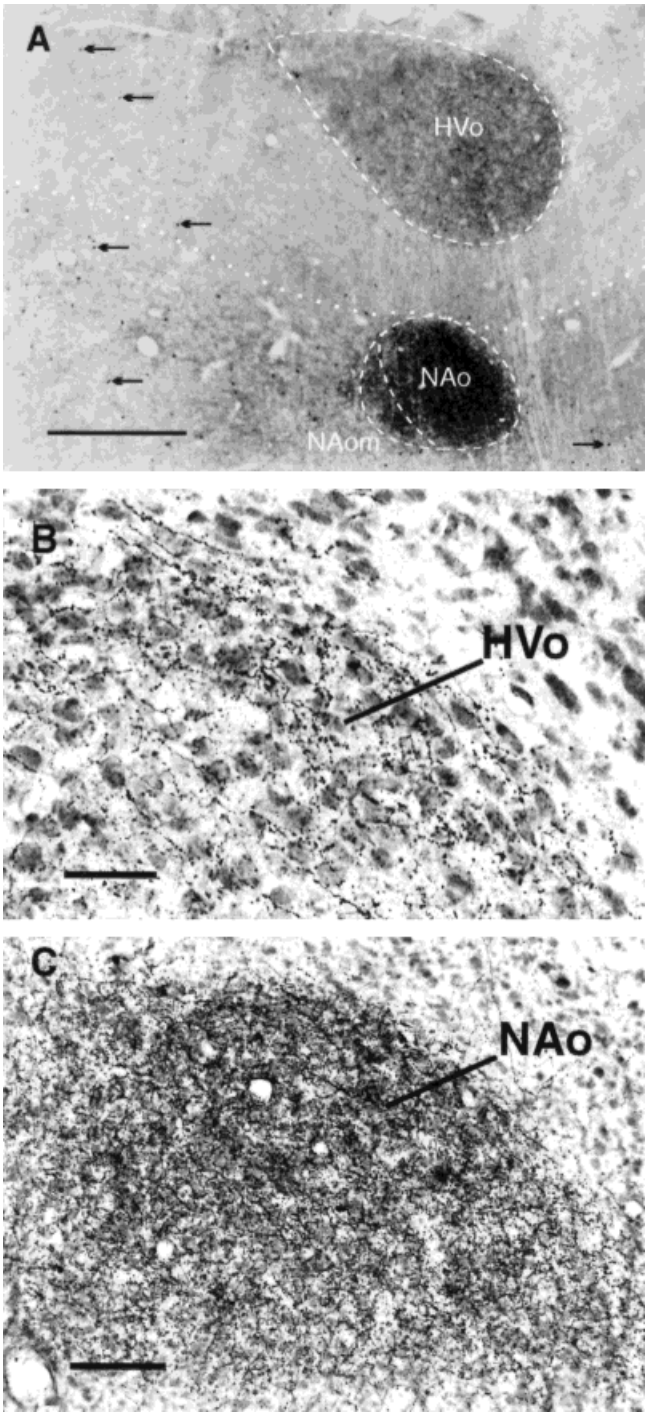

Fig. 9. **A:** Brightfield photomicrograph shows enkephalin-like immunoreactivity (ELI) staining within the oval nucleus of ventral hyperstriatum (HVo) and oval nucleus of anterior neostriatum (NAo). Dashed lines indicate nuclear boundaries defined by Nissl staining, and dotted line indicates the location of the hyperstriatal lamina (LH). Arrows indicate labeled somata external to the HVo and the NAo. Note that unstained fibers traversing the LH are also visible. **B:** High-power brightfield photomicrograph of the lateral HVo reveals ELI fibers in relation to Nissl-stained profiles. **C:** Brightfield photomicrograph of the NAo illustrates exceptionally high concentration of varicose fibers in this fiber plexus: Nissl-stained profiles are largely obscured by ELI fibers. Subjects were female in A, male in B and C. Scale bars = 500 μm in A, 50 μm in B, 100 μm in C.

Diencephalon

Within the thalamus, fiber densities were greatest within medial populations, including the lateral habenula and subhabenular nucleus and nucleus paramedians. Many perinuclear "shell" regions also exhibited high levels of reactivity. Among these regions were the shell of the nucleus ovoidalis, the surround of the nucleus rotundus

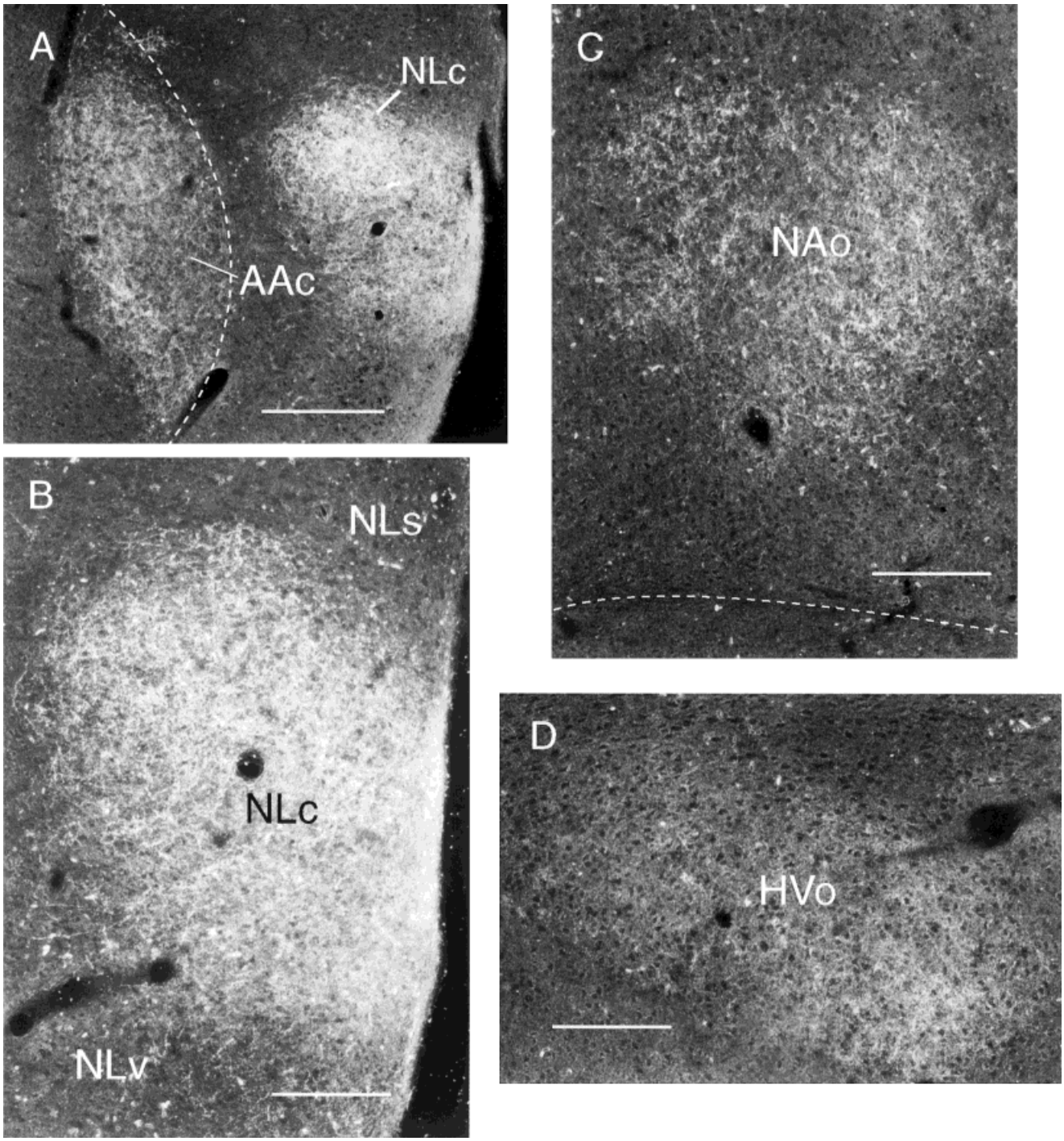

Fig. 10. Darkfield photomicrographs of enkephalin-like immunoreactivity (ELI) fiber patterns in the vocal control nuclei (VCN) of a nestling. **A:** ELI staining within the central nucleus of lateral neostriatum (NLc) and the anterior nucleus of anterior archistriatum (AAc). Dashed line indicates the location of the fiber tract dorsal archistriatal lamina (LAD). The relative location of ELI fiber plexuses is similar to that of the adult, although the pattern of fiber labeling in the NLc is somewhat different (see text). **B:** Higher power photomicrograph of fiber staining in the nestling NLc. **C:** ELI fibers within the nestling oval nucleus of anterior neostriatum (NAo) exhibit a different distribution than in adults (see text). Dashed line indicates the fiber tract dorsal medullary lamina (LMD). **D:** ELI fibers within the nestling oval nucleus of ventral hyperstriatum (HVo) are distributed most densely within its lateral portion, as in adults (see Fig. 9). Scale bars = 500 μm in A, 250 μm in B–D.

(Rt; Fig. 16B), and the nuclei of the dorsal posterior thalamus. Of the latter cell groups, the intermediate and lateral nuclei of the posterodorsal thalamus (DIP and DLP, respectively) also contained low-to-moderate densities of centrally located, varicose axons; similar fibers were also present within the medial pole of the DMP. Some fiber

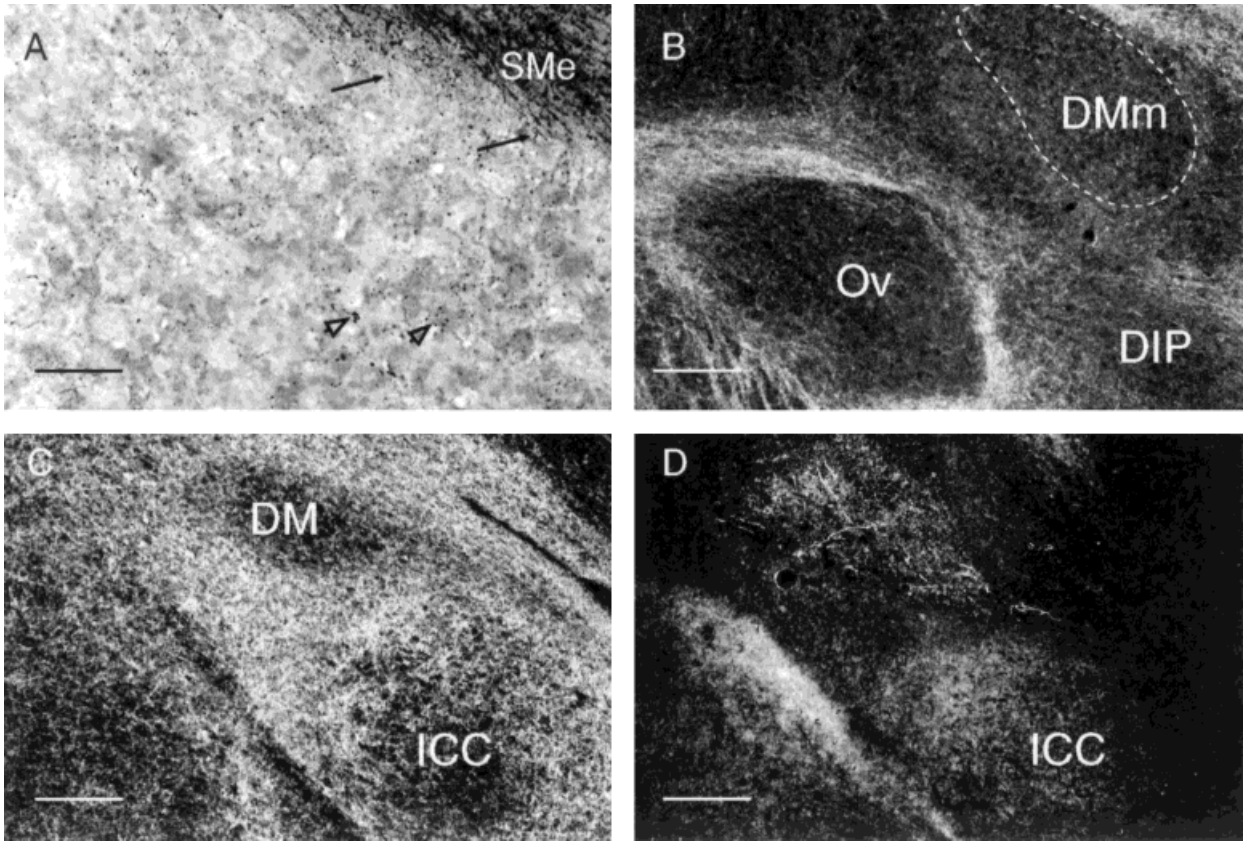

Fig. 11. **A:** Brightfield photomicrograph illustrates fine, varicose, ELI fibers extending from the stria medullaris (SMe) into the thalamic vocal nucleus (magnocellular nucleus of the dorsomedial thalamus; DMm). Arrows indicate fibers, the left arrowhead indicates a varicose fiber segment, and the right arrowhead indicates a somal profile associated with puncta. **B:** Darkfield photomicrograph illustrates the relative density of ELI fiber distribution in the thalamus, including the magnocellular nucleus of dorsomedial thalamus (DMm), the auditory nucleus (the ovoid nucleus of the thalamus [Ov] and the dorsointermediate nucleus of the posterior thalamus [DIP]). Note the reactive fibers in the SMe at the upper right. **C:** Darkfield photomicrograph of ELI fibers within the auditory midbrain, including the central nucleus of the inferior colliculus (ICC) and the vocal control nucleus (dorsomedial nucleus of the nucleus intercollicularis; DM). **D:** Darkfield photomicrograph for comparison with C. Fibers within the DM were labeled from a tracer injection into the AAc (see text). Subject was male in A–D. Scale bars = 50 μm in A, 200 μm in B–D.

tracts contained exceptionally high densities of reactive fibers: the stria medullaris, the septomesencephalic tract, and the tractus ovoidalis, the latter being continuous with reactive fields within the ovoidalis shell and the nucleus paramedians. Moderate fiber densities were contained within the lateral part of the dorsolateral nucleus of the anterior thalamus and the lateral portion of the nucleus of the septomesencephalic tract.

All regions of the preoptic area and hypothalamus contained a dense network of labeled fibers. Reactive perikarya were also present within these areas. Surprisingly few reactive perikarya were found within the ovoidalis shell (Durand et al., 1992, 1993) and only in the caudoventral portion. The ventral thalamus contained a sparsely scattered population of labeled cells interspersed among the fiber bundles of the OM and immediately medial to the OM. This region is identified as Campi Forelli in pigeons (Karten and Hodos, 1967) and may be homologous to the mammalian zona incerta, which contains proenkephalin (Harlan et al., 1987) and through which the ansa lenicularis projects. Labeled somata were also present within the peripretectal nucleus (peri-PT) field and were oriented parallel to the perimeter of this nucleus.

Mesencephalon

Cell groups surrounding the tectal ventricle contained high levels of reactive fibers. These included the periventricular gray region (SGP; Fig. 14D), the external nucleus of the inferior colliculus (ICX), and the medial margin of the inferior colliculus (ICM; for terminology, see Knudsen, 1983; Durand et al., 1993). The ICX and, to lesser degree, the ICM also contained reactive cell bodies. The area between the DM and the central nucleus of the inferior colliculus (ICC; see Fig. 11C) contained an exceptionally dense field of terminal labeling and may correspond to the apparently enkephalin-rich core and shell portions of the intercollicular region, as identified in the chick (Puelles et al., 1994). Reactive somata were distributed medial to the highly reactive intercollicular shell region and appeared roughly continuous with the population of labeled somata within the ventral thalamus (see above). Coarse and fine varicose fibers were distributed orthogonal to the tectal perimeter within central layers of the tectum. Many of

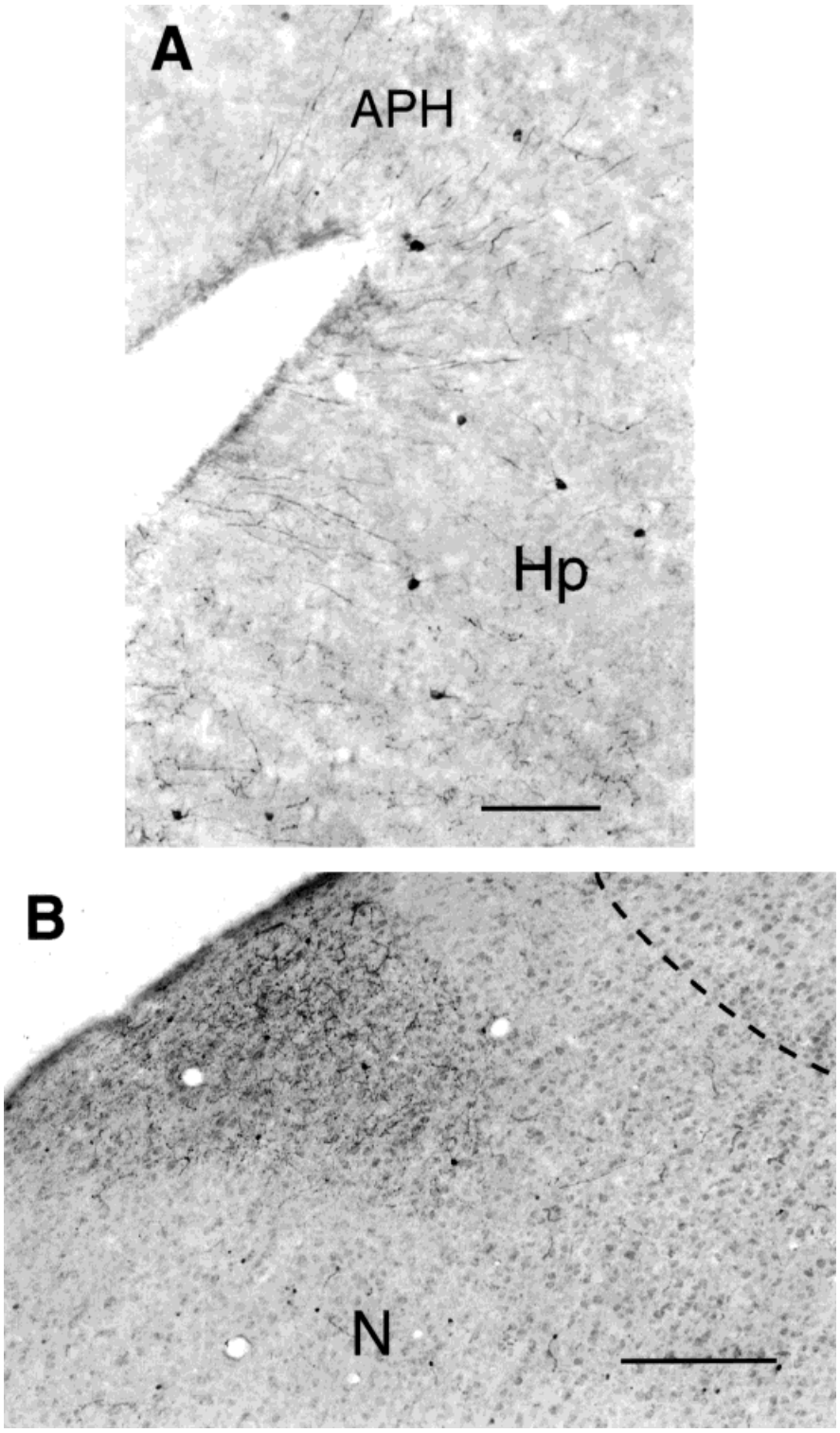

Fig. 12. **A:** Brightfield photomicrograph illustrates ELI somata and fibers within the hippocampus (Hp) and the area parahippocampus (APH). **B:** Brightfield photomicrograph of a small ELI fiber plexus within the lateral neostriatum (N). Dashed line indicates the hyperstriatal lamina (LH). Subjects were female in A, male in B. Scale bar = 100 μm in A, 250 μm in B.

these fibers appeared to form terminal sprays of fibers in tectal layer 3. The core of the ICC was largely devoid of reactivity. A loosely organized network of reactive fibers extended from the ventral perimeter of ICC into the subadjacent reticular formation and from the intercollicular region into the periaqueductal gray. The dorsomedial

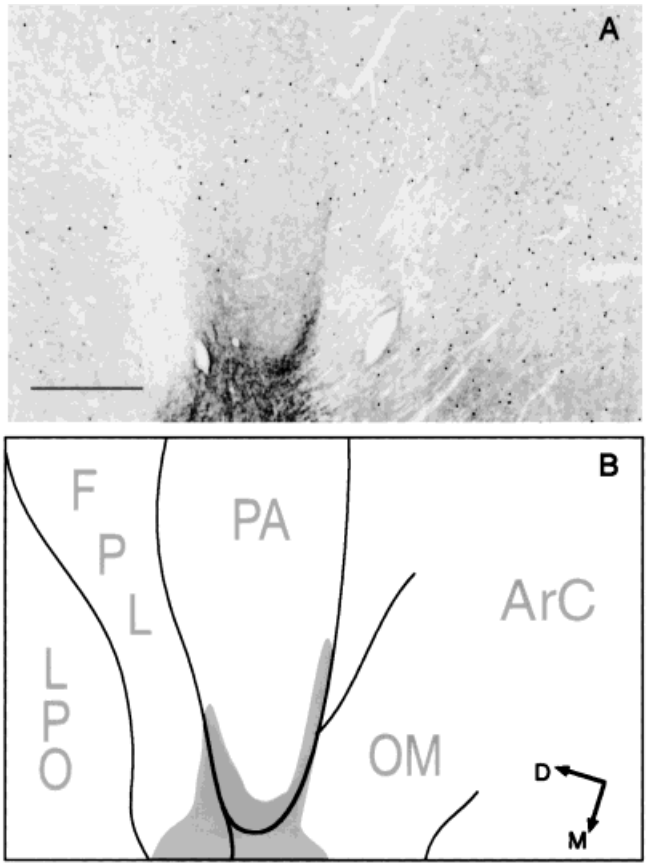

Fig. 13. **A:** Brightfield photomicrograph illustrates somal ELI label in the archiastriatum centrale (ArC) relative to neural populations of the basal ganglia (PA, paleostriatum augmentatum; LPO, lobus parolfactorius). Note that stained somata are more numerous within the ArC than within the PA or LPO. Dark staining along the ventrolateral border of the PA indicates a cluster of reactive somata and fibers. **B:** Schematic drawing showing the cytoarchitectonic boundaries between the ArC, the PA, the lateral forebrain bundle (FPL), and the LPO for the photomicrograph in Figure 12A. Subject was female. Scale bar = 500 µm.

margin of the SGP field was continuous with the peri-PT field, and its medial margin was continuous with fibers that extended from the large (25–30 µm), reactive somata that composed the bulk of the lateral spiriform nucleus SpL. The isthmic nuclei were largely devoid of reactivity, although an occasional reactive, varicose fiber traversed these cell groups. Catecholaminergic cell groups, including the area ventralis of Tsai, substantia nigra, and locus ceruleus, contained reactive fiber fields.

Neural connections of ELI neurons in VCN revealed with double-labeling methods

Tissue sections from a previous study utilizing the tracer biocytin (Durand et al., 1997) were stained for ELI to obtain additional information about the connections of enkephalin-immunoreactive neurons and fibers in vocal control pathways (see Materials and Methods). Biocytin injections into the AAc retrogradely label cells within the NLc. Subsequent staining for ELI (Fig. 17A) reveals that NLc neurons projecting to the AAc are encapsulated with ELI-reactive fibers. The morphology of these reactive fibers resembles the basket-like clusters within the NLc described above.

After a biocytin injection into the ventral periphery of the lateral HVo (Durand et al., 1997; Fig. 11), retrogradely labeled cells were observed within the NAom. Subsequent staining for ELI revealed large, reactive boutons clustered along the primary and secondary dendrites of the biocytin-filled cells (Fig. 17B). No perisomal, immunoreactive elements were observed. However, if they were present, it would have been difficult to visualize such elements due to intense staining of the somata of retrogradely filled cells within the NAom. It is noteworthy that basket-like clusters were not observed within the NAom in cases in which no filled cells were present in the nucleus (see above).

Injection of biocytin into the thalamic nucleus, DMm (see Fig. 4 in Durand et al., 1997), yielded both lightly and darkly stained magnocellular neurons (≥30 µm) within LPOm. After mENK immunocytochemistry, no reactive fibers were found to be associated with the back-filled somata. Although the dendrites of back-filled cells were sometimes adjacent to reactive fibers, these processes did not appear to contact one another (Fig. 17C). The absence of any obvious association between the LPOm projection neurons and the immunoreactive fibers was also suggested by examination of counterstained material (Fig. 17D): Immunostained varicose fibers and puncta were most abundant over small to medium-sized profiles (7–25 µm). Cells of this size were never labeled from tracer injections into the DMm or its surround (Durand et al., 1997).

The distribution of reactive fibers within the LPOm also sharply contrasts with the distribution of biocytin-labeled axons of LPOm projection neurons filled from biocytin injections into the DMm. Axon collaterals of these retrogradely labeled cells could be traced to nearby magnocellular neurons, some of which were also retrogradely labeled from the DMm. The collaterals from a single retrogradely filled cell could sometimes be traced to more than one neighboring magnocellular neuron, where the axon appeared to form axosomatic contacts. Thus, many magnocellular somal profiles within the portion of the LPOm that contained back-filled cells were encapsulated with dense clusters of large boutons (Fig. 17E).

DISCUSSION

Summary and conclusions

The overall distribution of ELI in the budgerigar brain resembled patterns of ELI reported for other avian species in many respects, with one notable exception (see Evolutionary Considerations, below): Like the songbird pallium (zebra finch: Ryan et al., 1981; Bottjer and Alexander, 1995; European starling and song sparrow: Ball et al., 1988), the most extensive fields of ELI were associated with forebrain VCN. In both budgerigars and songbirds, ELI was also present within the medial anterior neostriatum (Bottjer and Alexander, 1995) and along the lamina that separates the anterior HV and HD (ELI that is also present in domestic chickens; Reiner et al., 1984b). In addition, the zebra finch and budgerigar both express ELI to some degree within the parahippocampal region, lateral neostriatum, and medial archistriatum (see Fig. 2 in Bottjer and Alexander, 1995). The budgerigar paleostriatum and archistriatum exhibited unique patterns of ELI with respect not only to other birds but also to other vertebrates studied to date, including the caiman (Brauth, 1984), the turtle (Reiner, 1987), and mammals (for re-

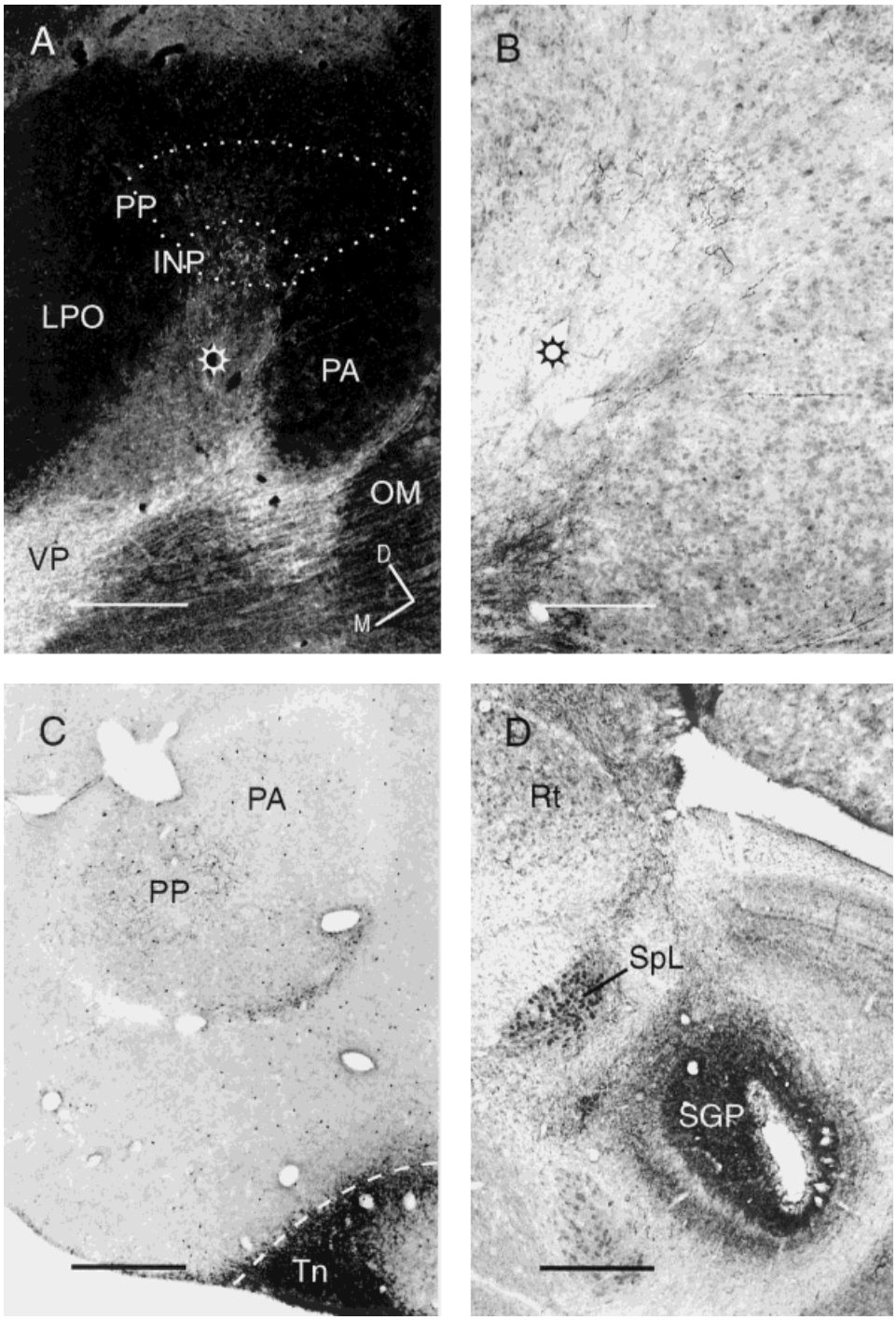

Fig. 14. **A:** Darkfield photomicrograph illustrates ELI staining within paleostriatal fields, including the paleostriatum augmentatum (PA), the primitive paleostriatum (PP), the intrapeduncular nucleus (INP), the lobus parolfactorius (LPO), and the ventral paleostriatum (VP). Dotted outline indicates the boundary of a large-celled region. **B:** The same tissue at higher magnification in brightfield (star indicates the same tear artifact as the star in A); note the negligible fiber staining within the PP and sparse distribution of stained fibers in the INP. **C:** Brightfield photomicrograph illustrates ELI staining at the caudal pole of the paleostriatum, including the PA and PP. Note the concentration of reactive somata and fibers along the ventrolateral border of the PA and the relatively low density of stained fibers in the PP vs. the Tn. **D:** Brightfield photomicrograph of Nissl-stained tissue illustrates intense ELI staining of neurons of the lateral spiriform nucleus (SpL) and of the periventricular gray substance of the tectum (SGP). Subjects were male in A, B, and D, female in C. Scale bars = 500 μm in A, 250 μm in B, 500 μm in C,D.

views, see Reiner et al., 1984a; Graybiel, 1990; Medina and Reiner, 1995). Immunocytochemistry for mENK in the budgerigar, as discussed below, yielded little evidence of a well-defined striatopallidal enkephalinergic projection, although the pattern of ELI supported both the presence of striatonigral projection and a projection from the SpL onto

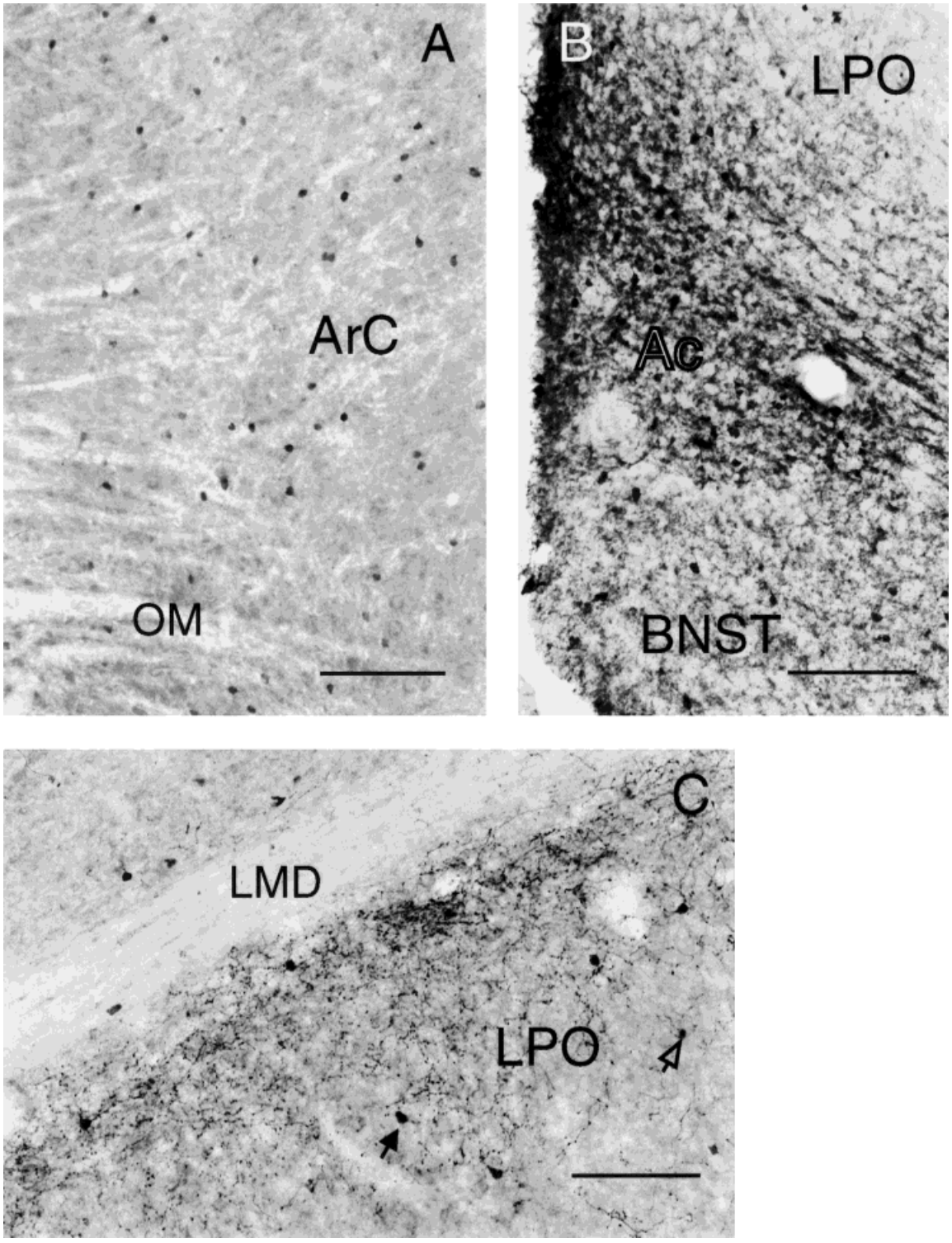

Fig. 15. Brightfield photomicrographs of ELI in archistriatal and paleostriatal populations. **A:** Numerous stained somata are present among the fiber bundles of the occipitomesencephalic tract (OM) tract associated with the archiastriatum centrale (ArC). **B:** The nucleus accumbens (Ac) and the bed nucleus of the stria terminalis (BNST) can be distinguished on the basis of unique patterns of ELI. **C:** In the dorsal lobus parolfactorius (LPO), stained fiber fields and somata form an "end zone" immediately caudal to the ELI plexus of the magnocellular nucleus of lobus parolfactorius (LPOm); note the large size of somata (solid arrow) within the fiber plexus relative to somata outside this region (open arrow). Subject was female. Scale bars = 250 μm.

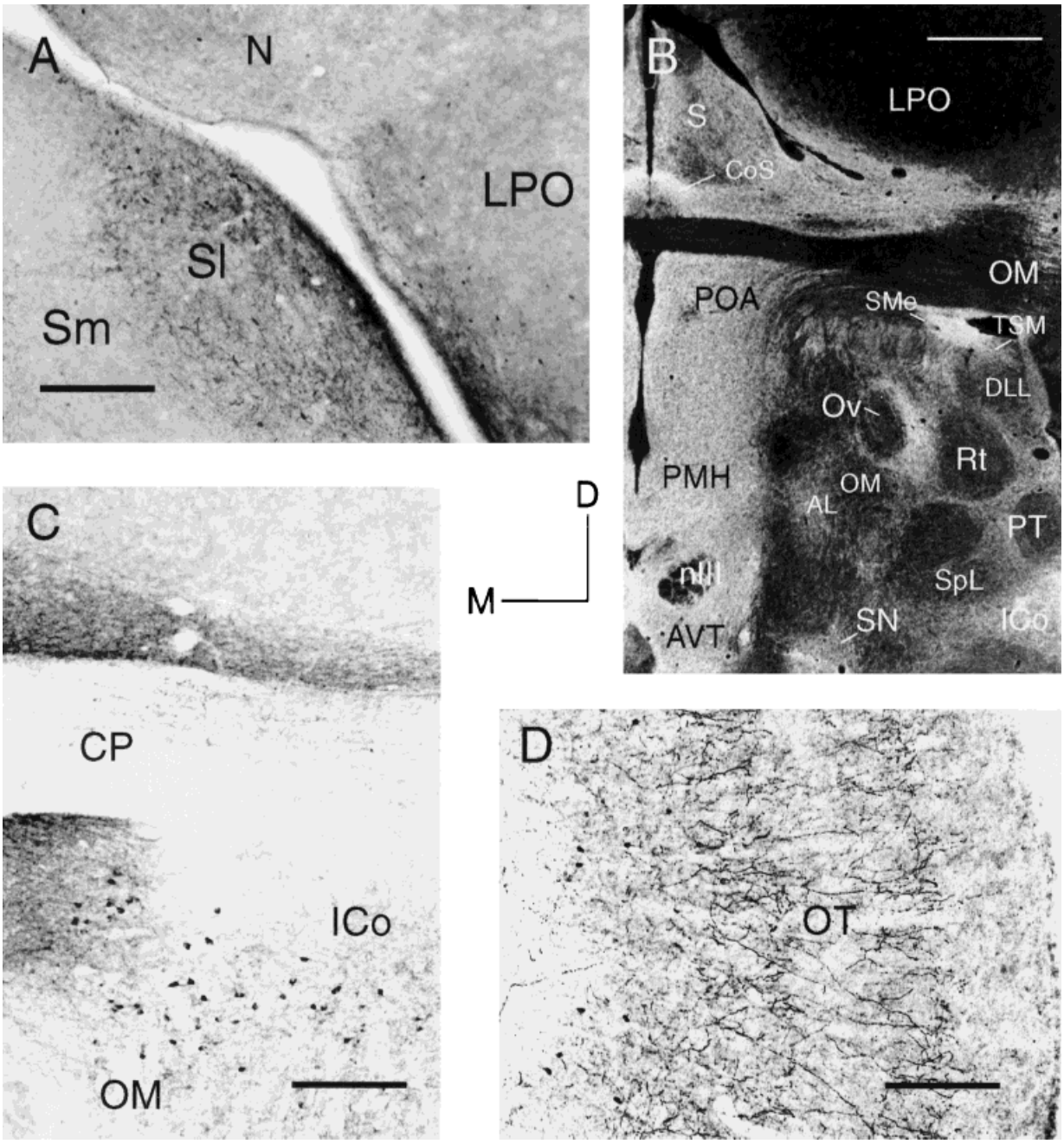

Fig. 16. **A:** Brightfield photomicrograph shows relative ELI staining within the septal nuclei and the adjacent lobus parolfactorius (LPO). **B:** Darkfield photomicrograph shows ELI staining patterns within the central thalamus, preoptic area, and ventral tegmental area (see text). **C:** Brightfield photomicrograph illustrates reactive fibers and somata within central regions of the midbrain at the level of the posterior commissure. **D:** Brightfield photomicrograph of reactive somata and fibers within the deep and superficial layers, respectively, of the tectum. Subjects were male in A and B, female in C and D. For abbreviations, see list. Scale bars = 250 μm in A,C,D, 1.0 mm in B.

the optic tectum. Whereas low levels of ELI were present within the budgerigar PA and PP, the budgerigar archistriatum contained high levels of both reactive cells and fibers. The continuity of archistriatal ELI with the lateral VCN (AAc and NLc) raises the possibility that the archistriatum contributes to ELI within these premotor nuclei of the budgerigar song system. Similarly, basal forebrain cell groups may contribute to ELI within the anterior VCN (NAo and HVo) given the presence of what appeared to be ascending reactive fibers within the LPOm that crossed the LMD at the level of the NAo. Although these fibers could have been descending into the LPOm, the latter is less likely given the relative paucity of NAo somal labeling and given the high levels of reactive cells within a region of the LPO that was continuous with the LPOm reactive field.

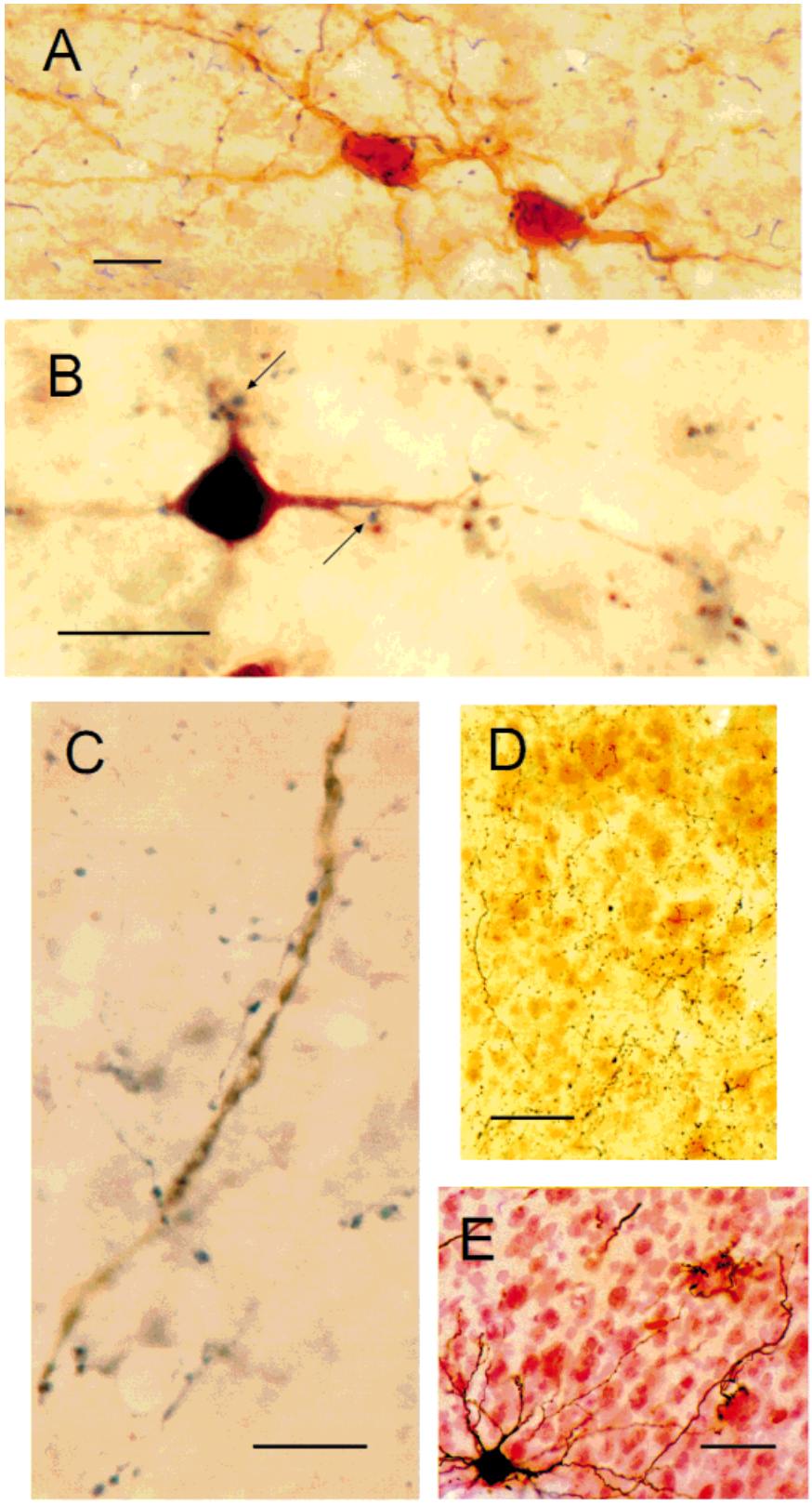

Fig. 17. Brightfield photomicrographs of double-labeled material (A–C). Brown stain (diaminobenzidine; A,C) or red stain (VIP chromagen; see B) indicates biocytin label transported from injection sites within either the AAc (A), HVo (B), or DMm (C); blue stain (SG chromogen) indicates reactive elements. In D and E, tissue was counterstained with neutral red to visualize the cytoarchitecture of the LPOm relative to stained fibers. **A:** Two cells in the dorsal NLc are back filled from a biocytin injection into the AAcd and are encapsulated with reactive fiber clusters or "baskets." **B:** A projection neuron in the NAom back filled from an injection within the ventral border of the HVo is shown in relation to ELI puncta (arrows). **C:** A dendrite of an LPOm projection neuron back filled from the DMm is shown in relation to ELI fibers that appear to make few or no synaptic contacts (see text). **D:** ELI fibers coursing through the dorsal LPOm are least dense in the vicinity of magnocellular projection neurons. **E:** An LPOm magnocellular projection neuron back filled from the DMm extends axon collaterals that ramify onto nearby magnocellular cell bodies, a pattern of innervation that contrasts with the relative absence of immunostained fibers surrounding these large projection neurons. Subjects were male in A and E, female in B–D. Scale bars = 20 µm in A,C, 10 µm in B, 50 µm in D,E.

VCN

Of particular interest was the specific reactivity of the budgerigar VCN and associated end zones: Budgerigar and songbird pallial VCN are not believed to be homologous (Streidter, 1994; Durand et al., 1997). In light of the present study, however, it is clear that VCN of both budgerigars and oscines contain conspicuous enkephalinergic fiber labeling, whereas most of the surrounding pallium is devoid of immunoreactive terminal fields. In species for which vocal learning has not been documented, ELI within the pallium either has not been reported (pigeon: Bayon et al., 1980; domestic chick: de Lanerolle et al., 1981) or is rare (domestic chicken: Reiner et al., 1984b).

A finer level of analysis of ELI distribution also revealed some striking similarities across songbird VCN (as defined by zebra finches, starlings, and song sparrows) and budgerigar VCN. In both cases, the vocal nucleus of the subventricular lateral neostriatum (NLc of budgerigars, high vocal center or HVC of songbirds) contains ELI fibers that surround neuronal somata in basket-like arrangements (Ryan et al., 1981; Ball et al., 1988; Bottjer and Alexander, 1995). In both songbird species and budgerigars, the archistriatal nucleus efferent to the vocal lateral neostriatum (AAc in budgerigars, nucleus robustus archistriatalis [RA] in songbirds) is characterized by high densities of reactive somata (Ball et al., 1988; Bottjer and Alexander, 1995), a greater density of reactive fibers within its margins than within its core, and ELI fibers that extend from the nucleus into the neighboring neostriatum (Bottjer and Alexander, 1995). The vocal control region of the rostrolateral LPO (LPOm in budgerigars, Area X in songbirds) contains unbranched fiber segments, occasional sprays of varicose fibers, and scattered punctate labeling (Bottjer and Alexander, 1995). In both oscines and budgerigars, the ELI field that encompasses the vocal control nucleus of the anterior neostriatum (NAom in budgerigars, the lateral magnocellular nucleus of the anterior neostriatum [LMAN] in songbirds) extends beyond the Nissl-defined boundaries of the nucleus in coronal sections, although the portion of the field coextensive with the nucleus is exceptionally dense (Ball et al., 1988; Bottjer and Alexander, 1995).

Thus, although the budgerigar "song" system comprises a hyperstriatal nucleus (HVo) with no obvious anatomical counterpart in the songbird brain (Durand et al., 1997), and the archistriatal and neostriatal VCN are not considered to be homologous to those of oscines (Streidter, 1994), the telencephalic vocal nuclei of a parrot and of songbirds appear to be selectively innervated by enkephalin-like terminals of similar morphology. The evolution of common features in nonhomologous but functionally comparable systems suggests that opioid modulation of neural activity may be uniquely advantageous for socially based motor learning.

What is the source of enkephalinergic fibers in the VCN? Ryan et al. (1981) suggested that enkephalinergic input could be extrinsic to vocal control populations based on the absence perikaryal staining within songbird VCN in their study. Successful visualization of reactive somata within songbird VCN by Ball et al. (1988) led to their hypothesis that intrinsic interneurons could be the source of ELI fields within the VCN, although they did not discount the possibility that enkephalinergic innervation could arise from other sources.

The continuity of reactive fiber fields of the budgerigar VCN with subpallial populations of reactive somata and the absence of consistently higher densities of reactive somata within VCN relative to surrounding regions are both consistent with the existence of an external source of ELI innervation. In the zebra finch, ELI fibers were also followed across both the archistriatal lamina and the LMD into the overlying pallium (Bottjer and Alexander, 1995). Evidence also exists from tract-tracing studies that the VCN may receive input from ELI-rich areas of the ventral striatopallidum: Tracer injections into the AAc and the HVo labeled cells within the fiber fascicles of the lateral forebrain bundle and medial to this region (see Figs. 7 and 10 in Durand et al., 1997). Additional double-labeling experiments with complementary fluorescent tracers and antisera could address the question of whether an extrinsic source of enkephalinergic input into the VCN via pathways arising from the basal forebrain is likely to exist. It may be that vocal control pathways for learning evolved in association with brain systems that mediate motivation and reward (Ryan et al., 1981).

Given the similarity of ELI distribution between the budgerigar and oscine telencephalic VCN, differences in ELI patterns within the diencephalon and mesencephalon were unexpected. In the budgerigar, the thalamic vocal nucleus, DMm, was notable for its relatively low density of ELI fibers; whereas, in zebra finches, the medial division of the dorsolateral thalamic nucleus (DLM) has been reported to contain a dense field of reactive terminations that is coincident with DLM nuclear boundaries (Bottjer and Alexander, 1995). Low levels of reactivity comparable to the budgerigar DMm have also been reported for the DMP in pigeons (Veenman et al., 1997) and chickens (de Lanerolle et al., 1981). These same studies also identified the DLM as low in reactivity. Thus, the songbird DLM may represent a specialized case. It is noteworthy that the DMm may support a functional role that is distributed between several thalamic nuclei in the songbird vocal system. Although the DLM, like the DMm, projects to a nucleus in the anterior neostriatum (Okuhata and Saito, 1987; Bottjer et al., 1989), it does not project directly upon premotor cell groups as is the case for the DMm (Durand et al., 1997).

The mesencephalic vocal nucleus, DM, in songbirds has been reported to lie within a region of dense ELI (Ball et al., 1988; Bottjer and Alexander, 1995), an observation that is consistent with the data presented here. However, previous reports did not distinguish the DM from surrounding fiber fields as a region of reduced reactivity. It is possible that the degree of intensification that was achievable with silver-gold impregnation (see Materials and Methods) permitted regional differences in fiber densities to be visualized more clearly than in previous studies. It is also possible that the distribution of reactive fibers in this region may indeed differ in budgerigars from that in oscines. It is noteworthy that the apparent innervation of the DM by AAc axons is weak (Streidter, 1994), unlike the robust projection of the RA upon the DM (Vicario, 1991).

Functional considerations

A striking feature of the ELI pattern within the budgerigar VCN was the large perikaryal fiber arrangement, especially within the ventral NLc. Basket-like fibers were demonstrated to encapsulate NLc projection neurons that project to the AAc (Fig. 17A). Basket-like ELI also charac-

terizes the songbird nuclei HVC and LMAN (Ryan et al., 1981; Ball et al., 1988; Bottjer and Alexander, 1995). However, perikaryal baskets were absent within the juvenile budgerigar NLc despite the presence of abundant reactive fibers and, as revealed in Nissl-stained material, neuronal clusters.

At 3 weeks of age, budgerigars have not yet acquired learned and acoustically complex contact calls (Farabaugh et al., 1994; Brittan-Powell et al., 1997; Hall et al., 1997). Juvenile calls at 3 weeks are relatively long and harsh sounding and consist of simple, repeating segments (Brittan-Powell et al., 1997; Hall et al., 1997). Lesions of the AAc, the target of NLc projection neurons, prior to 3 weeks of age have little effect on call structure (Heaton and Brauth, 1996). However, birds that sustain AAc lesions as nestlings never successfully produce contact calls or warble song as they mature, indicating that pathways involving the AAc and NLc are necessary for producing learned, frequency-modulated vocalizations. The lateral VCN of a 3-week-old bird may not yet be providing the control over vocal output that is critical later to producing learned sounds. It is possible that, as the nestling matures, developmental changes in enkephalinergic innervation of the NLc, such as the appearance of clusters of reactive boutons around the cell bodies of NLc projection neurons, contribute to increasingly organized patterns of vocal motor activity that appear around the time of fledgling. Results of studies that examine the action of mENK at the cellular level bear upon this question: Exogenous application of mENK has been shown to facilitate electrical coupling of neuronal activity and has been hypothesized to function in the coordination of motor patterns (Dyakanova et al., 1993). Furthermore, mENK has been demonstrated to act synergistically with acetylcholine (Xu and Gintzler, 1992), which appears to be present in both the budgerigar NLc and the songbird HVC (Ryan et al., 1981; Ball et al., 1990; Cookson et al., 1996). It is also noteworthy that, given the role of "practice" in the gradual acquisition of learned motor patterns, evidence exists suggesting that peptide cotransmission depends on intense or repetitive presynaptic activity (for review, see Martinez et al., 1990).

Paleostriatum and archistriatum

The pattern of ELI innervation within the budgerigar paleostriatal complex did not conform to the pattern common to other amniote classes studied to date (Medina and Reiner, 1995). Specifically, populations that comprise the avian dorsal striatum (LPO and PA; with the exception of the LPOm, its end zone, and the medial margin of the LPO) and the primary population of the dorsal pallidum (PP) were characterized by low levels of reactivity. Negligible fiber labeling was present throughout the extent of the PP except for a restricted region within the caudal pole of this cell group, in which low-to-moderate fiber density was observed. Even here, the reactive field was not confined to the boundaries of the PP but extended into the surrounding PA. Within the nucleus interpeduncularis (INP), fiber density approached that of the PP caudal pole. In both a songbird (Bottjer and Alexander, 1995) and other avian species (Reiner et al., 1984b; Anderson and Reiner, 1990), the PP is richly innervated by a dense ELI field that appears to arise, as in mammals, from the surrounding striatum (Karten and Dubbeldam, 1973). In addition, the cellular reactivity within the PA of previously studied avian species is readily distinguishable from the negligible to nonexistent cellular label of the overlying pallium. Finally, the INP is unreactive in these other species. Thus, the pattern of ELI distribution within the budgerigar dorsal striatopallidum is unique in several respects, although the differences cited above were largely in degree and not in kind.

The discrepancy between the ELI distribution in the budgerigar basal ganglia vs. the basal ganglia of other species studied to date was confined to the dorsal, or sensorimotor, paleostriatal complex (Medina and Reiner, 1995; Veenman et al., 1995). The pattern of ELI within the budgerigar ventral striatum, ventral pallidum, and efferent populations of the PP (Karten and Dubbeldam, 1973; Reiner et al., 1982) was similar to what has been reported previously (de Lanerolle et al., 1981; Reiner et al., 1982, 1984b; Bottjer and Arnold, 1997).

In contrast to the relative paucity of ELI within the dorsal paleostriatal complex, the budgerigar archistriatum was rich in ELI. The high density of somal labeling relative to the adjacent pallium in the budgerigar was reminiscent of descriptions pertaining to paleostriatal labeling in the chicken, a species that apparently exhibits negligible archistriatal ELI (Reiner et al., 1984b). In the zebra finch, reactive fibers and somata have been observed within the archistriatum (Bottjer and Alexander, 1995), and a photomicrograph (Fig. 7C of Bottjer and Alexander, 1995) suggests the possibility that reactive fibers within the medial pole of the zebra finch archistriatum, the Tn (Stokes et al., 1974), may be continuous with the fiber field within the dorsomedial margin of the RA. If this is true, then this pattern of archistriatal ELI in a finch would be similar to the archistriatal ELI in the budgerigar, in which the AAc reactive field is continuous with fields of the caudomedial archistriatum, the presumptive budgerigar Tn. Nonetheless, the density of reactive elements in the budgerigar archistriatum apparently far exceeds levels observed in the zebra finch or in any other avian species studied to date.

Evolutionary considerations

The histochemical properties of the amniote basal ganglia have been analyzed in species of birds, reptiles, and mammals and have been found to be quite similar in all cases of amniotes, suggesting that the evolution of the basal ganglia in amniotes has been very conservative (for review, see Medina and Reiner, 1995). A histochemical property thought to be present in amphibians and cartilaginous fishes as well as in mammals and birds is the existence of striatal enkephalinergic neurons with terminations in the pallidum. This characteristic appears to be much reduced in the budgerigar dorsal striatum, at least with respect to methionine ELI.

Staining for leucine and mENK, both of which derive from preproenkephalin, has indicated that the patterns of ELI for the two neuropeptides are similar within the dorsal striatum of the chicken and pigeon (Reiner et al., 1984; Anderson and Reiner, 1990). Thus, it is unlikely, although not inconceivable, that ELI within the budgerigar dorsal striatum would be more abundant if a leucine enkephalin-specific antiserum had been employed. Furthermore, different lots of primary antibody were used in the present study, and these came from the same supplier that provided the primary antiserum for a study of ELI in male zebra finches (Bottjer and Alexander, 1995; Incstar Corp.). The birds exhibited high levels of cellular label within the

PA and LPO, high levels of fiber labeling within the PP, and cellular staining within the archistriatum that was comparable to the overlying pallium, consistent with results obtained from pigeons and domestic chickens (see Fig. 5B in Bottjer and Alexander, 1995). Finally, only the dorsal striatopallidum (PA, PP, and most of LPO) of the budgerigar exhibited unusually low ELI: Ventral regions of the striatopallidum and other nuclei of the basal forebrain and mesencephalon exhibited patterns of ELI consistent with other studies. In sum, it is unlikely that the pattern of ELI within the budgerigar striatopallidum reflects the staining methodology of visualization employed in this study.

If they are confirmed, then the unusually high levels of reactivity within the budgerigar archistriatum, in conjunction with the reduced reactivity of somatomotor regions of the paleostriatal complex, may point to a derived pattern of enkephalinergic pathways within the budgerigar motor system. Such a notion cannot be readily dismissed: Recent observations by Wild et al. (1997) have uncovered the existence of novel somatosensory pathways in the budgerigar that are associated with a complete somatotopic representation of the body within the nucleus basalis. Prior tract-tracing studies have demonstrated that basalis neurons project to neostriatal cell groups afferent to the archistriatum (Wild et al., 1985; Dubbeldam and Vissar, 1987). The archistriatum is not only a major source of extratelencephalic premotor efferents (Zeier and Karten, 1971), but it projects to the somatomotor paleostriatal complex (Veenman et al., 1995). Taken together, the results of the present study and those of previous studies of vocal control pathways (Streidter, 1994; Durand et al., 1997), auditory pathways (Brauth and McHale, 1988; Streidter, 1994; Farabaugh and Wild, 1997), and somatosensory pathways (Wild et al., 1997) indicate that unusual neural specializations have evolved in budgerigars and perhaps in other psittacines that may contribute to their exceptional ability to learn and use complex communication sounds on a continuous basis.

ACKNOWLEDGMENTS

The authors thank Ms. Naheed Vatcha for her excellent technical assistance and Ms. Sharon Egender for her conscientious animal care. This research was supported (in part) by research grant 5 F32 DC 00105-03 from the National Institute for Deafness and Communication Disorders (NIH) to S.E.D. and by research grant MH 40698 from the National Institute of Mental Health (NIH) to S.E.B.

LITERATURE CITED

Anderson, K.D. and A. Reiner (1990) Extensive co-occurrence of substance P and dynorphin in striatal projection neurons: An evolutionarily conserved feature of basil ganglia organization. J. Comp. Neurol. *295:*339–369.

Ball, G.F. (1990) Chemical neuroanatomical studies of the steroid sensitive-songbird vocal control system: A comparative approach. In J. Balthazart (ed): Hormones, Brain and Behavior in Vertebrates, Vol. 8. Basel: Karger, pp. 148–167.

Ball, G.F. (1994) Neurochemical specializations associated with vocal learning and production in songbirds and budgerigars. Brain Behav. Evol. *44:*234–246.

Ball, G.F. and Casto, J.M. (1991) Autoradiographic location of NMDA receptors in the avian song control system using [^{3}H] MK-801. Soc. Neurosci. Abstr. *17:*1053.

Ball, G.F., P.L. Farris, B.K. Hartmen, and J.C. Wingfield (1988) Immunohistochemical localization of neuropeptides in the vocal control regions of two songbird species. J. Comp. Neurol. *268:*171–180.

Ball, G.F., B. Nock, J.C. Winfield, B.S. McEwen, and J. Balthazart (1990) Muscarinic cholinergic receptors in the songbird and quail brain: A quantitative autoradiograpic study. J. Comp. Neurol. *298:*431–442.

Banta, P.A. and I.M. Pepperberg (1995) Learned English vocalizations as a model for studying the budgerigar (*Melopsittacus undulatus*) warble song. Soc. Neurosci. Abstr. *21:*964.

Bayon, A., L. Koda, E. Battenberg, R. Azad, and F.E. Bloom (1980) Regional distributions of endorphin, met^5-enkephalin and leu^5-enkephalin in the pigeon brain. Neurosci. Lett. *16:*75–80.

Bottjer, S.W. and A. Alexander (1995) Localization of met-enkephalin and vasoactive intestinal polypeptide in the brains of male zebra finches. Brain Behav. Evol. *45:*153–177.

Bottjer, S.W. and A.P. Arnold (1997) Developmental plasticity in neural circuits for a learned behavior. Annu. Rev. Neurosci. *20:*459–482.

Bottjer, S.W., E.A. Missener, and A.P. Arnold (1984) Forebrain lesions disrupt development but not maintenance of song in passerine birds. Science *224:*901–902.

Bottjer, S.W., K.A. Halsema, S.A. Brown, and E.A. Misener (1989) Axonal connections of a forebrain nucleus involved with vocal learning in zebra finches. J. Comp. Neurol. *279:*312–326.

Brauth, S.E. (1984) Enkephalin-like immunoreactivity within the telencephalon of the reptile *Caiman crocodilus*. Neuroscience *2:*345–358.

Brauth, S.E. and C.M. McHale (1988) Auditory pathways in the budgerigar II. Intratelencephalic pathways. Brain Behav. Evol. *32:*193–207.

Brittan-Powell, E.F., R.J. Dooling, and S.M. Farabaugh (1997) Vocal development in budgerigars (*Melopsittacus undulatus*): Contact calls. J. Comp. Psychiatr. *111:*226–241.

Cookson, K.K., W.S. Hall, J.T. Heaton, and S.E. Brauth (1996) Distribution of choline acetyltransferase and acetylcholinesterase in vocal control nuclei of the budgerigar (*Melopsittacus undulatus*). J. Comp. Neurol. *369:*220–235.

de Lanerolle, N.C., R.P. Elde, S.B. Sparber, and M. Frick (1981) Distribution of methionine-enkephalin immunoreactivity in the chick brain: An immunohistochemical study. J. Comp. Neurol. *199:*513–533.

Dubbeldam, J.L. and A.M. Visser (1987) The organization of the nucleus basalis-neostriatum complex of the mallard (*Anas pltyrhynchosl*) and its connections with the archistriatum and the paleostriatium complex. Neuroscience *21:*487–517.

Durand, S.E., J.M. Tepper, and M.F. Cheng (1992) The shell region of the nucleus ovoidalis: A subdivision of the avian auditory thalamus. J. Comp. Neurol. *323:*495–518.

Durand, S.E., M.X. Zuo., S.L. Zhou, and M. Cheng (1993) Avian auditory pathways show met-enkephalin-like immunoreactivity. Neuroreport *4:*727–730.

Durand, S.E., J.T. Heaton, and S.E. Brauth (1996) Common organization features in budgerigar and oscine forebrain vocal control. Soc. Neurosci. Abstr. *22:*1402.

Durand, S.E., J.T. Heaton, S.K. Amateau, and S.E. Brauth (1997) Vocal control pathways through the anterior forebrain of a parrot (*Melopsittacus undulatus*). J. Comp. Neurol. *377:*179–206.

Dyakonova, T.L., L.L. Moroz, and W. Winlows (1993) Effects of met–enkephalin on electrical coupling between identified neurons in the pulmonate snails *Helix* and *Lymnea*. Comp. Biochem. Physiol. *106C:*93–101.

Farabaugh, S.M. and J.M. Wild (1997) Reciprocal connections between primary and secondary auditory pathways in the telencephalon of the budgerigar (*Melopsittacus undulatus*). Brain Res. *747:*18–25.

Farabaugh, S.M., A. Linzenbold, and R.J. Dooling (1994) Vocal plasticity in budgerigars (*Melopsittacus undulatus*): Evidence for social factors in the learning of contact calls. J. Comp. Psychol. *108:*81–92.

Gahr, M., H.R. Güttinger, and D.E. Kroodsma (1993) Estrogen receptors in the avian brain: Survey reveals general distribution and forebrain areas unique to songbirds. J. Comp. Neurol. *327:*112–122.

Gramza, A.F. (1970) Vocal mimicry in captive budgerigars (*Melopsittacus undulatus*). Z. Tierpsychol. *27:*971–983.

Graybiel, A.M. (1990) Neurotransmitters and neuromodulators in the basal ganglia. Trends Neurosci. *13:*244–254.

Hall, W.S., K.K. Cookson, J.T. Heaton, T. Roberts, S.D. Shea, and S.E. Brauth (1997) Audio-vocal learning in budgerigars. Ann. N.Y. Acad. Sci. *807:*352–367.

Harlan, R.E., B.D. Shivers, G.J. Romano, R.D. Howells, and D.W. Pfaff (1987) Localization of preproenkephalin mRNA in the rat brain and spinal cord by in situ hybridization. J. Comp. Neurol. *258:*159–184.

Heaton, J.T. and S.E. Brauth (1996) Effects of vocal archistriatal lesions and early deafening on vocal development in the budgerigars. Soc. Neurosci. Abstr. *22:*694.

Karten, H.J. (1968) The ascending auditory pathway in the pigeon (*Columba livia*). II. Telencephalic projections of the nucleus ovoidalis thalami. Brain Res. *11:*134–153.

Karten, H.J. and J.L. Dubbeldam (1973) The organization and projections of the paleostriatal complex in the pigeon (*Columbia livia*). J. Comp. Neurol. *148:*61–90.

Karten, H.J. and W. Hodos (1967) A Stereotaxic Atlas of the Brain of the Pigeon (*Columbia livia*). Baltimore, MD: Johns Hopkins Press.

Kitt, C.A., C. Hohman, J.T. Coyle, and D.L. Price (1994) Cholinergic innervation of mouse forebrain structures. J. Comp. Neurol. *341:*117–129.

Knudsen, E.I. (1983) Subdivisions of the inferior colliculus in the barn owl (*Tyto alba*). J. Comp. Neurol. *218:*174–186.

Konishi, M. (1994) An outline of recent advances in birdsong neurobiology. Brain Behav. Evol. *44:*279–285.

Margoliash, D., E.S. Fortune, M.L. Sutter, A.C. Yu, B.D. Wren-Hardin, and A. Dave (1994) Distributional representation in the song system of oscines: Evolutionary implications and functional consequences. Brain Behav. Evol. *44:*247–264.

Marler, P. (1991) Song-learning behavior: The interface with neuroethology. Trends Neurosci. *14:*199–206.

Martinez, J.L., Jr., P.H. Janak, S.B. Weinberger, G. Schucteis, and D.E. Derrick (1990) Enkephalinergic influences on behavioral and neural plasticity: Mechanisms of action. In L. Erinoff (ed): Neurobiology of Drug Abuse: Learning and Memory, Monograph 97. Rockville, MD: NIDA Research, pp. 48–78.

Medina, L. and A. Reiner (1995) Neurotransmitter organization and connectivity of the basal ganglia in vertebrates: Implication for the evolution of basal ganglia. Brain Behav. Evol. *46:*235–258.

Nottebohm, F. (1991) Reassessing the mechanisms and origins of vocal learning in birds. Trends Neurosci. *14:*206–211.

Nottebohm, F., T.M. Stokes, and C.M. Leonard (1976) Central control of song in the canary, *Serinus canarius*. J. Comp. Neurol. *165:*457–486.

Okuhata, S. and N. Saito (1987) Synaptic connections of thalamo-cerebral vocal nuclei in the canary. Brain Res. Bull. *18:*35–44.

Paton, J.A., K.R. Manogue, and F. Nottebohm (1981) Bilateral organization of the vocal control pathway in the budgerigar (*Melopsittacus undulatus*). J. Neurosci. *1:*1279–1288.

Pepperberg, I.M. (1988) The importance of social interaction and observation in the acquisition of communicative competence: Possible parallels between avian and human learning. In T.R. Zentall and B.G. Galef (eds): Social Learning: A Comparative Approach. Hillsdale, NJ: Erlbaum, pp. 279–299.

Pepperberg, I.M., K.J. Brese, and B.J. Harris (1991) Solitary sound play during acquisition of English vocalizations by an African Gray parrot (*Psittacus erithacus*): Possible parallels with children's monologue speech. Appl. Psychol. *12:*151–178.

Puelles, L., C. Robles, T. Martínez-de la Torrre, and S. Martínez (1994) New subdivision schema for the avian torus semicircular: Neurochemical maps in the chick. J. Comp. Neurol. *340:*98–152.

Reiner, A. (1987) The distribution of proenkephalin-derived peptides in the central nervous system of turtles. J. Comp. Neurol. *259:*65–91.

Reiner, A., H.J. Karten, and N.C. Brecha (1982a) Enkephalin-mediated basal ganglia influences over the optic tectum: Immunohistochemistry of the tectum and the lateral spiriform nucleus in pigeon. J. Comp. Neurol. *208:*37–53.

Reiner, A., S.E. Brauth, and H.J. Karten (1984a) Evolution of the amniote basal ganglia. Trends Neurosci. *7:*320–325.

Reiner, A., B.M. Davis, N.C. Brecha and H.J. Karten (1984b) The distribution of enkephalinlike immunoreactivity in the telencephalon of the adult and developing chicken. J. Comp. Neurol. *228:*245–262.

Reiner, A., S.E. Brauth, C.A. Kitt, and R. Quirion (1989) Distribution of mu, delta, and kappa opiate receptor types in the forebrain and midbrain of pigeons. J. Comp. Neurol. *280:*359–382.

Ryan, S., A.P. Arnold, and R.E. Elde (1981) Enkephalin-like immunoreactivity in vocal control regions of the zebra finch brain. Brain Res. *229:*236–240.

Scharff, C. and F. Nottebohm (1991) A comparative study of the behavioral deficits of various parts of the zebra finch song system: Implications for vocal learning. J. Neurosci. *11:*2896–2913.

Sibley, C.G. and J.E. Ahlquist (1990) The Phylogeny and Classification of Birds. New Haven, CT: Yale University Press.

Stokes, T.C., C.M. Leonard, and F. Nottebohm (1974) The telencephalon, diencephalon, and mesencephalon of the canary, *Serinus canaria*, in the stereotaxic coordinates. J. Comp. Neurol. *156:*337–374.

Striedter, G.F. (1994) The vocal control pathways in budgerigars differ from those in songbirds. J. Comp. Neurol. *343:*35–56.

Veenman, C.L., J.M. Wild, and A. Reiner (1995) Organization of the avian "corticostriatal" projection system: A retrograde and anterograde pathway tracing study in pigeons. J. Comp. Neurol. *354:*87–126.

Veenman, L.C., L. Medina, and A. Reiner (1997) Avian homologues of mammalian intralaminar, mediodorsal and midline thalamic nuclei: Immunohistochemical and hodological evidence. Brain Behav. Evol. *49:*78–98.

Vicario, D.S. (1991) Organization of the zebra finch song control system: II. Functional organization of outputs from nucleus robustrus archistriatalis. J. Comp. Neurol. *309:*486–494.

Wild, J.M., and J.A. Arends (1987) A respiratory-vocal pathway in the brainstem of the pigeon. Brain Res. *407:*191–194.

Wild, J.M., J.A. Arends, and P.H. Zeigler (1985) Telencephalic connections of the trigeminal system in the pigeon (*Columba livia*): A trigeminal sensorimotor circuit. J. Comp. Neurol. *22:*441–464.

Wild, J.M., H. Reinke, and S.M. Farabaugh (1997) A nonthalamic pathway contributes to a whole body map in the brain of the budgerigar. Brain Res. *755:*137–141.

Xu, H. and A.R. Gintzler (1992) Opioid enhancement of evoked [met^5] enkephalin release requires activation of cholinergic receptors: Possible involvement of intracellular calcium. Proc. Natl. Acad. Sci. USA *89:*1978–1982.

Zeier, H. and H.J. Karten (1971) The archistriatum of the pigeon: Organization of afferent and efferent connections. Brain Res. *31:*313–326.